# The structure of the end-Cretaceous dinosaur fossil record in North America

#### **Highlights**

- The probability of detecting dinosaurs decreases toward the end-Cretaceous
- Sampling intensity does not impact the probability of dinosaur detection
- Detection probability is driven by geologic outcrop and present-day land cover
- Geological sampling biases cloud our view of end-Cretaceous dinosaur diversity

#### **Authors**

Christopher D. Dean, Alfio Alessandro Chiarenza, Jeffrey W. Doser, ..., Paul J. Valdes, Richard J. Butler, Philip D. Mannion

#### Correspondence

christopher.dean@ucl.ac.uk

#### In brief

Dean et al. examine the fossil record of North American dinosaurs prior to the end-Cretaceous mass extinction. Estimates of detection probability from occupancy models decrease prior to the extinction event and are independent from sampling intensity, suggesting that geological biases obscure our understanding of their diversity dynamics.







#### **Article**

# The structure of the end-Cretaceous dinosaur fossil record in North America

Christopher D. Dean, 1,9,\* Alfio Alessandro Chiarenza, 1 Jeffrey W. Doser, 2 Alexander Farnsworth, 3,4 Lewis A. Jones, 1 Sinéad J. Lyster, 5 Charlotte L. Outhwaite, 6,7 Paul J. Valdes, 3,4 Richard J. Butler, 8 and Philip D. Mannion 1

<sup>1</sup>Department of Earth Sciences, University College London, 5 Gower Place, London WC1E 6BS, UK

#### **SUMMARY**

Whether non-avian dinosaurs were in decline prior to their extinction 66 million years ago remains a contentious topic. This uncertainty arises from spatiotemporal sampling inconsistency and data absence, which cause challenges in distinguishing between genuine biological trends and sampling artifacts. Consequently, there is an inherent interest in better quantifying the quality of the data and concomitant biases of the dinosaur fossil record. To elucidate the structure of this record and the nature of the biases impacting it, we integrate paleoclimatic, geographic, and fossil data within a Bayesian occupancy modeling framework to simultaneously estimate the probability of dinosaurs occupying and being detected in sites across North America throughout the latest Cretaceous for the first time. We find that apparent declines in occupancy generated from the raw fossil record do not match modeled occupancy probability, which generally remained stable throughout the latest Cretaceous. Instead, they coincide with decreased probability of detecting dinosaur occurrences, despite high overall sampling during this interval. By incorporating model covariates, we additionally reveal that detection probability is directly and significantly influenced by the available area of geological outcrop and modern land cover. Our findings offer evidence that traditional comparisons of diversity estimates between time intervals are likely inaccurate due to underlying structural issues in the geological record operating at both local and regional scales. This study underscores the utility of occupancy modeling as a novel approach in paleobiology for quantifying the impact of heterogeneous sampling on the available fossil record.

#### INTRODUCTION

The mass extinction event at the Cretaceous/Paleogene (K/Pg) boundary marks both the demise of the non-avian dinosaurs <sup>1,2</sup> and a critical interval in vertebrate evolution. <sup>3,4</sup> Although a bolide impact is now widely accepted as the principal extinction mechanism, there has been intense debate regarding the trajectory of dinosaur diversity and diversification patterns leading up to the K/Pg boundary. In particular, this argument centers on whether non-avian dinosaurs were already in long-term terminal decline due to changes in global environmental conditions, <sup>2,5–15</sup> with many studies focused on the rich latest Cretaceous (Campanian-Maastrichtian; ~83.6–66 Ma) dinosaur fossil record of North America. <sup>2,10,13,14,16–19</sup> Approximately 50% of reported latest Cretaceous global dinosaur occurrences are from the North American continent, <sup>19</sup> with the majority from the western

margin of the Western Interior Basin (WIB), a foreland basin flooded by an epeiric sea that divided North America into western (Laramidia) and eastern (Appalachia) subcontinents. Exhibiting precise temporal constraints, high levels of sampling, and a relatively continuous stratigraphic succession, 14,19-22 the WIB represents an unprecedented dataset for discerning patterns in dinosaur macroecology and macroevolution prior to the mass extinction. 16,23 A literal interpretation of this rich fossil record suggests a Campanian peak in dinosaur species richness, followed by a decline in the Maastrichtian. 11,14,16,18,19

However, a variety of authors have suggested that the apparent decline in diversity in the latest Cretaceous in the WIB might be an artifact of spatiotemporal sampling biases in the fossil record—specifically spatial and taphonomic shifts in the available sampling window 18,24—rather than a genuine reflection of biological processes. 18,19,24–29 Although the available fossil record provides



<sup>&</sup>lt;sup>2</sup>Department of Forestry and Environmental Resources, North Carolina State University, 2800 Faucette Dr., Raleigh, NC 27607, USA

<sup>&</sup>lt;sup>3</sup>School of Geographical Sciences, University of Bristol, University Rd., Bristol BS8 1SS, UK

<sup>&</sup>lt;sup>4</sup>State Key Laboratory of Tibetan Plateau Earth System, Environment and Resources, Institute of Tibetan Plateau Research, Chinese Academy of Sciences, No. 16 Lincui Road, Chaoyang District, Beijing 100101, China

<sup>&</sup>lt;sup>5</sup>Department of Geosciences, The Pennsylvania State University, Deike Building, University Park, PA 16802, USA

<sup>&</sup>lt;sup>6</sup>Centre for Biodiversity & Environment Research, University College London, Gower Street, London WC1E 6BT, UK

<sup>&</sup>lt;sup>7</sup>Institute of Zoology, Zoological Society of London, Regent's Park, London NW1 4RY, UK

<sup>&</sup>lt;sup>8</sup>School of Geography, Earth and Environmental Sciences, University of Birmingham, Edgbaston, Birmingham B15 2TT, UK

<sup>&</sup>lt;sup>9</sup>Lead contact

<sup>\*</sup>Correspondence: christopher.dean@ucl.ac.uk https://doi.org/10.1016/j.cub.2025.03.025



an unprecedented archive of biological information, it is now well established that heterogeneous sampling confounds our attempts to reconstruct macroevolutionary and ecological patterns through deep time. 30-32 The known fossil record is not an accurate reflection of genuine biological patterns but instead a product of spatiotemporal variation in underlying preservation potential as well as biases introduced from resultant sampling of that remaining record.33,34 These factors arise from a complex web of geological, 30,35 environmental, 36 and anthropogenic 37 processes, which vary across time, 38 geography, 39 depositional environment, 33,40 and among taxa. 41 In particular, spatial sampling heterogeneity-and, more broadly, spatial data absence-has increasingly been recognized by paleontologists as a significant driver of observed patterns in deep time and, more broadly, of our understanding of the fossil record. 34,42-49 Changes in the underlying sampling universe between time intervals, including the spatial extent of available data and the environments and preservational conditions associated with those data, leave the resulting record incomplete and significantly impact our ability to accurately infer a wide range of macroevolutionary patterns and processes.5

These issues have been suggested to particularly impact the North American dinosaur record prior to the K/Pg extinction. Chiarenza et al. 18 hypothesized that the formation of the proto-Rocky Mountains and subsequent retreat of the Western Interior Seaway (WIS) in the Maastrichtian led to environmental and geological conditions that were simultaneously geographically restricted and less conducive for dinosaur preservation. Distinct northern and southern peaks in sampling intensity have been highlighted for the Campanian, whereas the Maastrichtian exhibits a more latitudinally constrained band of sampling 18,24; these peaks emanate from geological formations with high preservation quality (including the Dinosaur Park Formation in Alberta, Canada) acting as hotspots of fossil recovery. 18,51 Under this scenario, reduced sediment fluxes and accommodation space in the Maastrichtian also caused the progressive loss of regions suitable for fossil preservation, such as coastlines and inner shelf areas, reducing the burial potential and enhancing the exhumation of newly accumulated sedimentary packages. 18 This geographic and taphonomic restriction of the available sampling window suggests that dinosaur preservation and subsequent detection were comparatively reduced in the Maastrichtian record compared with the Campanian, which has potentially skewed interpretations of dinosaur diversity dynamics. 18

The impacts of this heterogeneous sampling are most evident within studies using either occurrence-based<sup>10</sup> or phylogenetic<sup>5–7,15</sup> approaches to reconstructing diversification histories for dinosaurs, which have reported variable outcomes as to whether dinosaurs appeared to be in short-term<sup>10</sup> or longterm<sup>5</sup> decline or were thriving until the end of the Cretaceous.<sup>6</sup> Allen et al. 15 showed that this variability of outcomes is partially driven by assumptions made about sampling within the latest Cretaceous: models assuming a relationship between species richness dynamics and sampling frequency reported an increase in diversification rates, whereas ones that assumed no relationship reported an overall decline. 15 It is therefore clear that attempts to reconstruct the macroevolutionary patterns of North American dinosaurs in the lead-up to the K/Pg boundary are hindered without first understanding changes in the spatiotemporal sampling of the fossil record.<sup>29</sup> Accurately estimating sampling variation through time <sup>52,53</sup> and clarifying the structure of the latest Cretaceous fossil record are critical to discern the relative impact of sampling on our understanding of past life and, ultimately, for resolving outstanding questions regarding dinosaur macroevolution prior to their extinction.

Occupancy modeling, a hierarchical modeling approach developed for population ecology and conservation, presents a way to understand the structure of the fossil record by estimating the detection probability of taxa through time while explicitly incorporating their spatial distribution and data absence. 54,55 This methodology provides the probability that a taxonomic unit (e.g., a species) occupies a set of geospatial locations (=sites), while simultaneously estimating and accounting for imperfect detection of that taxon. Repeated attempts at observing the taxonomic unit at these geospatial locations (=visits) generate detection histories (i.e., how many times the species has been detected or not detected). When integrated within the occupancy modeling framework, these detection histories provide independent estimates for the overall probability of occupancy at those sites, as well as the probability that the taxon is detected at those sites.<sup>55</sup> Including covariates within both subsections of the model can additionally reveal the factors driving both the occupancy and detection probability for that taxon. Occupancy modeling shares some similarity with capture-mark-recapture approaches, 56 which have been applied to the fossil record (e.g., Schachat et al. 57), but is explicitly spatial in nature, capturing an additional key element of bias for paleontological studies.<sup>32</sup> Although occupancy is an established metric in palaeontology, <sup>58–60</sup> and the potential for occupancy modeling to address paleobiologic questions has been highlighted by ecologists given its unique ability to directly infer the dominant drivers on our detection of fauna in deep time, 55 it has only been sparingly applied to data from the fossil record. 61-65 Recent advances in occupancy modeling have also enabled a wider range of occurrence-record datasets to be analyzed, including citizen science<sup>66</sup> and historical/collections-based data.<sup>67-70</sup> These datasets closely mirror records obtained from large occurrence-based paleontological datasets that are opportunistically collected and lack a standardized data collection methodology. Occupancy modeling therefore represents a relevant and flexible approach for quantifying variations in sampling probability through time and the causes of apparent data absences in the fossil record.

Here, we use variants of Bayesian occupancy models to evaluate the structure of the latest Cretaceous dinosaur fossil record. By establishing estimates of occupancy and detection probability across North America for four major clades (Ankylosauridae, Hadrosauridae, Ceratopsidae, and Tyrannosauridae), these models reveal how our ability to detect dinosaurs changed throughout the latest Cretaceous and allow us to test the hypothesis that detection probability decreased prior to the K/Pg mass extinction due to environmental changes and shifts in spatiotemporal sampling. First, we compare estimates of occupancy and detection probabilities produced from our models against naive occupancy (i.e., the raw proportion of occupied sites versus total available sites) through time to establish differences between perceived and modeled patterns in the Campanian and Maastrichtian (Figure 1B) across four main time bins (Table S4). Second, we run occupancy models that directly incorporate

#### **Article**



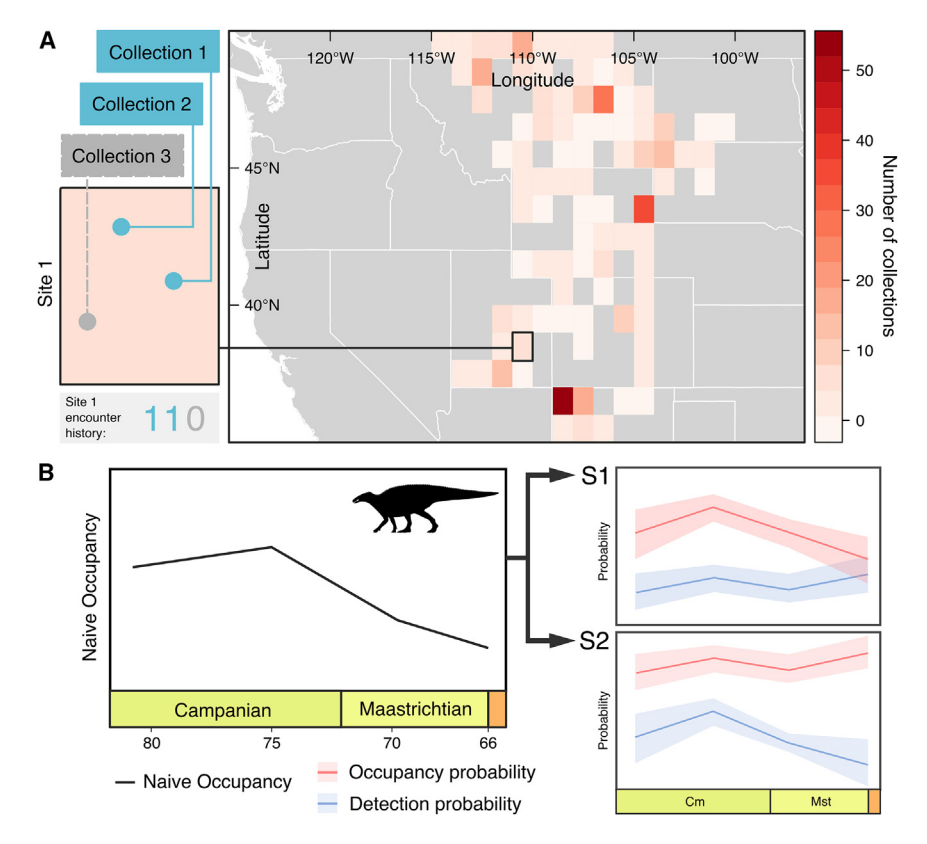


Figure 1. Occupancy modeling process and potential hypotheses

(A) Schematic describing the process for carrying out occupancy modeling on paleontological data from the Paleobiology Database (PBDB). The map shows dinosaur collections grouped into 1° × 1° resolution grid cells, designated as "sites." Within each site are collections containing fossil occurrences ("visits" under the occupancy framework). Collections containing the taxon of choice (blue boxes and dots) have a detection history of "1," noting that the taxon has been detected. Collections without the taxon of choice (gray box and dot) have a detection history of "0," noting that the taxon is undetected. Detection histories for all collections within a site are then tallied and used within the occupancy modeling framework.

(B) Schematic showing possible scenarios for occupancy and detection patterns prior to the Cretaceous/Paleogene (K/Pg) boundary. Naive occupancy of hadrosaurids (left) is shown to decrease throughout the latest Cretaceous. Scenario 1 (S1) shows occupancy probability decreasing, matching naive occupancy, and suggesting occupancy genuinely did decrease prior to the K/Pg boundary. Scenario 2 (S2) shows occupancy remaining stable and detection probability decreasing, suggesting that detection probability is driving observed occupancy patterns. Hadrosauridae silhouette produced by Matthew Dempsey, 2020, CC BY 3.0.

spatiotemporally explicit anthropogenic, geologic, and environmental covariates—including paleoclimatic model data, virtual taphofacies, <sup>18</sup> and present-day environmental and geographic data—to establish the main drivers impacting the detection of dinosaur fossil material across the latest Cretaceous. In assessing the structure and quality of the latest Cretaceous dinosaur fossil record under a unified framework, we endeavor to understand the processes that lead to the observed fossil record and which, in turn, influence our understanding of broadscale macroevolutionary patterns.

#### **RESULTS**

### Patterns in dinosaur families prior to the K/Pg mass extinction

Our results show that dinosaur families that exhibit a decline in naive occupancy (the raw proportion of sites occupied by a taxon) through time do not report convergent patterns in mean occupancy probability estimates (Figures 2 and 3). Ankylosauridae, Hadrosauridae, and Tyrannosauridae show an overall decline in naive occupancy through the latest Cretaceous between the first and last time bins ( $\sim 8\%$ ,  $\sim 9\%$ , and  $\sim 7\%$ , respectively, at  $0.5^\circ$  resolution; Figure 2, top row), although Hadrosauridae and Tyrannosauridae show a slight increase directly before the K/Pg boundary. By contrast, occupancy models optimized for opportunistically collected biological recording data ("sparta" models; see "occupancy modeling" section of STAR Methods for full details) show an overall increase for both clades in mean occupancy probability through time ( $\sim 13\%$ ,  $\sim 3\%$ ,

and  $\sim 9\%$ , respectively, at  $0.5^\circ$  resolution, comparing first and last bins; Figure 2, bottom row). Ceratopsidae shows an increase in both naive occupancy ( $\sim 30\%$  at  $0.5^\circ$  resolution) and occupancy probability ( $\sim 9\%$  at  $0.5^\circ$  resolution) between the first and last bins, with overall trajectories that match one another (Figure 2). Naive occupancy also severely underestimates occupancy probability, with large average differences between naive and probabilistic estimates for all clades (Ankylosauridae  $\sim 56\%$ , Hadrosauridae  $\sim 39\%$ , Ceratopsidae  $\sim 48\%$ , and Tyrannosauridae  $\sim 59\%$ ; all at  $0.5^\circ$  resolution).

Conversely, we find a stronger relationship between naive occupancy and trends in mean detection probability through time for clades in which naive occupancy decreases throughout the latest Cretaceous. Detection probabilities of Ankylosauridae, Hadrosauridae, and Tyrannosauridae show an overall decline toward the end-Cretaceous ( $\sim$ 5%,  $\sim$ 20%, and  $\sim$ 10%, respectively, at 0.5° resolution, comparing first and last bins at list length [LL] 4; Figure 2, bottom row), with Ankylosauridae and Hadrosauridae showing the largest decline prior to the K/Pg boundary, although Tyrannosauridae exhibit their largest overall decrease in the late Campanian. By contrast, detection probability for Ceratopsidae trends to an end-Maastrichtian peak (~4% overall average increase; Figure 2), while exhibiting a similar late Campanian low as Tyrannosauridae. Broadly similar trends in detection probability are also observed in results based on the best-fitting models of our multi-season (through time) spatially explicit occupancy models ("spOccupancy" models; see "occupancy modeling" section of STAR Methods for full details). However, detection probability for Tyrannosauridae shows



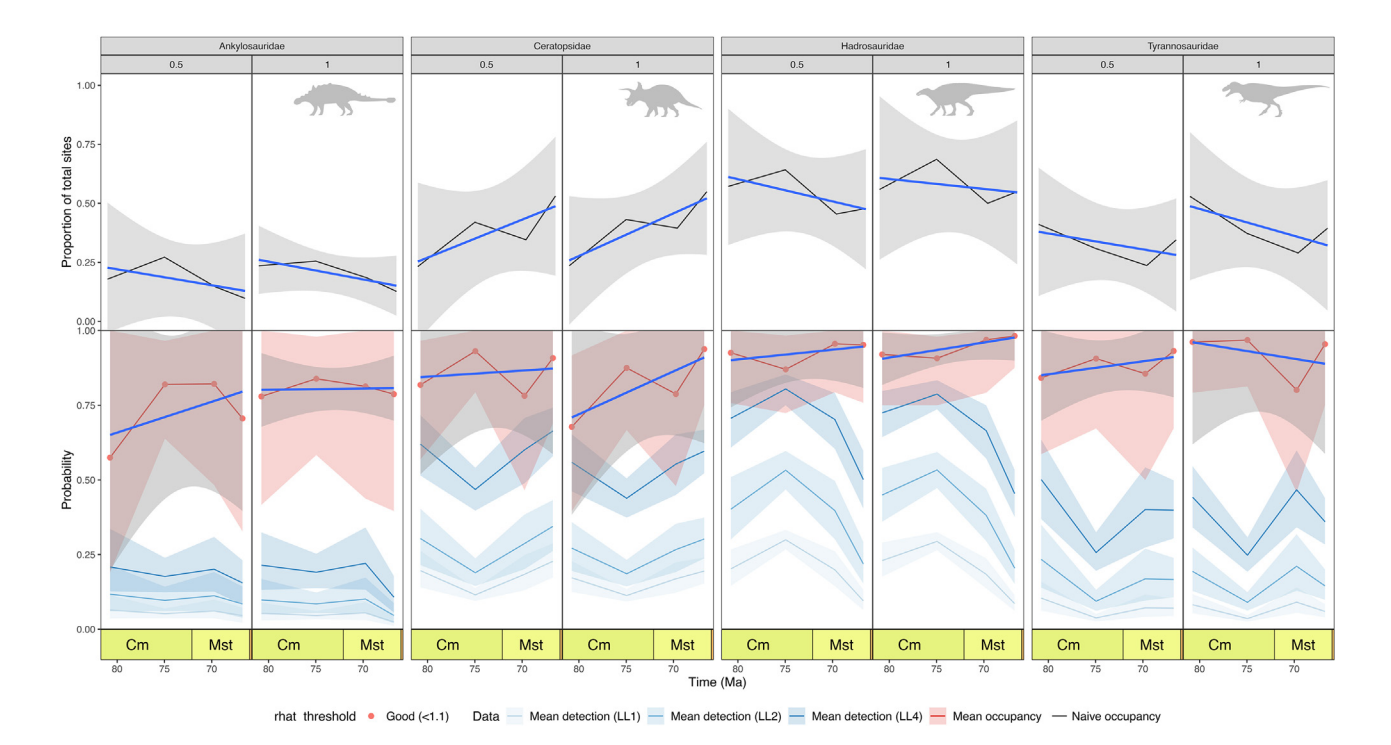


Figure 2. Naive occupancy and results from sparta models

Naive occupancy, as well as occupancy and detection probability estimates throughout the latest Cretaceous for dinosaur clades, presented at both  $0.5^{\circ} \times 0.5^{\circ}$  and  $1^{\circ} \times 1^{\circ}$  spatial resolution. Top row: naive occupancy estimate with associated trendline. Bottom: sparta estimated occupancy and detection probabilities, including trendline for occupancy probability. LL, list length (the number of genera within a collection); LL1, a single genus within a collection; LL2, 2–3 genera within a collection; LL4, 4+ genera within a collection. Shaded grey areas on the top and bottom rows represent the 95% confidence interval for trend lines. Colored shaded areas on the bottom row indicate BCIs (95%) for occupancy and detection probability. Ankylosauridae silhouette produced by Andrew Farke, 2013, CC BY 3.0; Hadrosauridae and Tyrannosauridae silhouettes produced by Matthew Dempsey, 2020, CC BY 3.0; Ceratopsidae silhouette produced by Ivan lofrida, 2024, CC BY 4.0.

See also Figures S1–S4 and S6 and Table S7.

a flat trajectory through time and Ankylosauridae shows both increases and decreases in detection probability prior to the K/Pg, depending on spatial resolution and the maximum number of visits (collections) used in the model (Figure 3) (see STAR Methods and Table S3 for further information).

These patterns in detection probability also remain broadly consistent at differing temporal (four time bins; six time bins) and spatial (0.5°  $\times$  0.5°; 1°  $\times$  1°) resolutions, and at different numbers of total visits (collections) per site (10 or 40) when using spatially explicit occupancy models (Figures 2, 3, and S1-S3). Overlapping 95% Bayesian credible intervals (BCIs) and similar trendlines indicate that varying spatiotemporal resolution does not substantially impact results for either occupancy or detection probability for any of the four clades in sparta models (Figures S1-S3) or detection probability for spOccupancy models (Figure 3). The 95% BCI also indicates that spatiotemporal resolution has a limited impact on precision, with lower spatial and temporal resolutions only showing a slight reduction in BCI width. Bayesian p values produced from posterior predictive checks also indicated adequate model fit across families, temporal binning scheme, spatial resolutions, and model types, except for Hadrosauridae at 0.5° × 0.5° resolution for formation bins (six time bins) using the sparta model, as well as Ankylosauridae at 0.5° × 0.5° resolution with maximum visits capped at 40 during the first time bin, Ceratopsidae at 1° × 1° with maximum visits capped at 40 during the second time bin, and Tyrannosauridae at 1 $^{\circ}$  × 1 $^{\circ}$  with maximum visits capped at 40 during the final time bin of the Maastrichtian, all using the spOccupancy model.

The geospatial arrangement of sampling can be more clearly examined within geographic projections of detection probability for dinosaur families produced from best-fitting models of our multi-season spatially explicit models (Figure 4). Projections show heightened detection probability that matches previously recognized hotspots of fossil recovery for certain clades and time intervals. Detection probability is high within southern Alberta, Canada, and Montana, USA, (~45°–55° latitude) during the Campanian for Hadrosauridae and throughout the available rock outcrop of the eastern WIB in the end-Maastrichtian for Ceratopsidae. Ankylosauridae and Tyrannosauridae show no clear hotspots of increased detection probability across any time interval, aside from isolated grid cells.

Our results also highlight clear differences between dinosaur lineages. Under both modeling approaches, the average detection probability across all four time intervals is highest overall for Hadrosauridae and lowest for Ankylosauridae (Figures 2 and 3). Patterns can also be observed in detection LL, a measure of the number of genera within sampled collections (Figure 2). A LL of four or greater (LL4; >3 genera within a collection) consistently shows the highest probability of detection, with a LL of 1 (a single



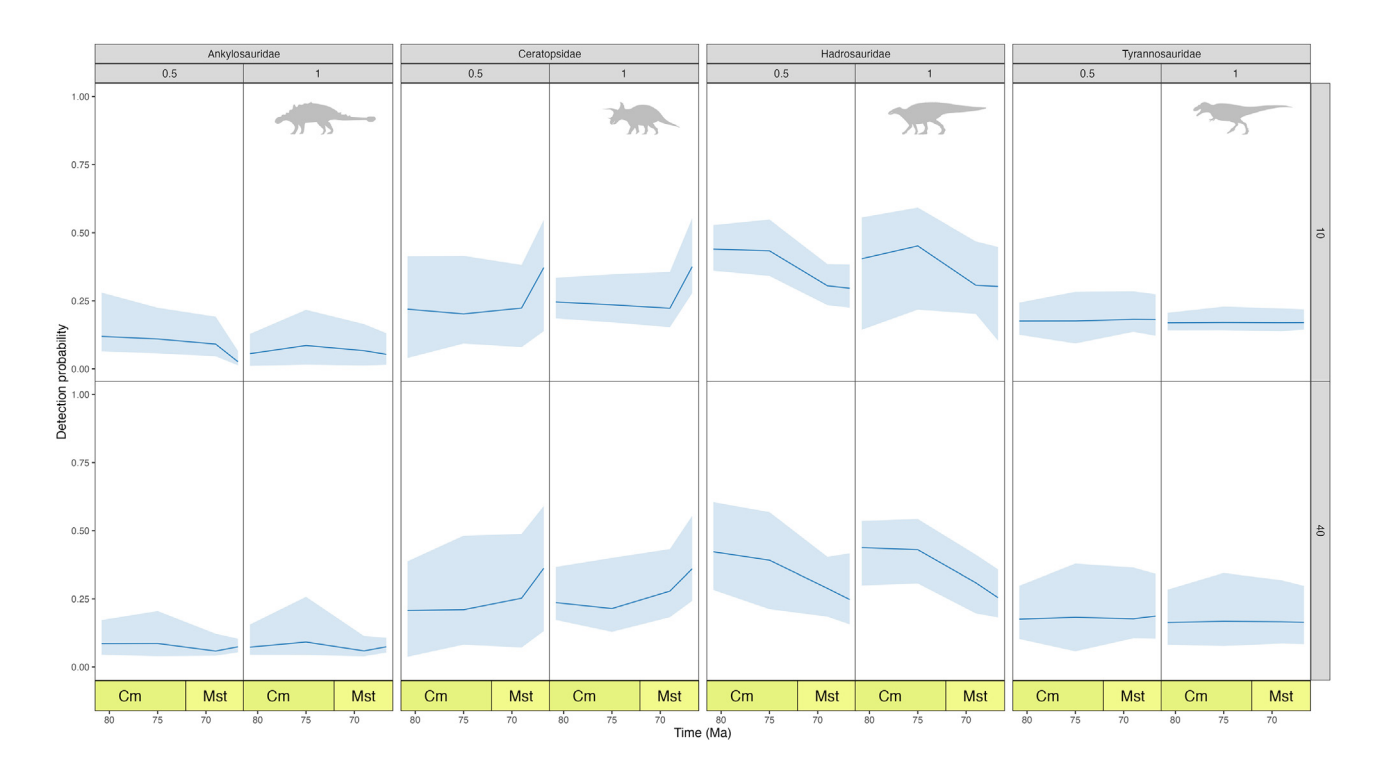


Figure 3. Detection probability from spOccupancy models

Detection probability for dinosaur clades throughout the latest Cretaceous generated from best-fitting models of multi-season spatially explicit Bayesian models run using spOccupancy, presented at both  $0.5^{\circ} \times 0.5^{\circ}$  and  $1^{\circ} \times 1^{\circ}$  spatial resolution (top categories) and with the maximum number of visits capped at 10 and 40 (right-hand side categories). Shaded areas represent BCIs (95%). Ankylosauridae silhouette produced by Andrew Farke, 2013, CC BY 3.0; Hadrosauridae and Tyrannosauridae silhouettes produced by Matthew Dempsey, 2020, CC BY 3.0; Ceratopsidae silhouette produced by Ivan Iofrida, 2024, CC BY 4.0. See also Figure S6 and Table S8.

genus within a collection) showing the lowest. There is only a small difference in mean detection probability between LLs of 1 and 2 (2–3 genera within a collection) for Ankylosauridae, Ceratopsidae, and Tyrannosauridae, with LL4 showing a distinctly higher score (Figure 2). Hadrosauridae detection probability shows more even differences between varying LLs (Figure S4).

#### **Drivers of occupancy and detection**

Several covariates representing geologic and geographic factors have statistically significant effects on the detection probability of dinosaur families within multi-season occupancy models (Figures 5 and 6; Table 1; full results reported in Table S1). Increased area of geological outcrop per grid cell impacts a total of three clades, showing a positive effect on detection probability at a variety of resolutions when visits to sites were capped at a maximum of 40 (at  $0.5^{\circ}$  resolution: Ceratopsidae:  $\beta = 0.24$ , 95% BCI = 0.061–0.417; Hadrosauridae:  $\beta$  = 0.288, 95% BCI = 0.141– 0.433; at 1° resolution: Ankylosauridae:  $\beta$  = 0.262, 95% BCI = 0.001-0.528). Land cover also appears in the best-fitting models of these three clades, showing a significant negative effect on Ankylosauridae detection within present-day open terrain (10 max. visits,  $0.5^{\circ}$ :  $\beta = -0.989$ ; 95% BCI = -1.757 to -0.258; 1°:  $\beta = -1.303$ , BCI = -2.252 to -0.371), a significant negative effect for detection of Ceratopsidae in present-day forested terrain  $(0.5^{\circ}, 10 \text{ max. visits: } \beta = -1.314; 95\% \text{ BCI} = -2.391 \text{ to } -0.325;$ 40 max. visits:  $\beta = -1.289$ ; 95% BCI = -2.444 to -0.234), and a significant positive effect for detection of Hadrosauridae in present-day forested terrain (1°, 10 max. visits:  $\beta$  = 0.742; 95% BCI = 0.022-1.482). Time bin categories appear as a covariate in the best-fitting models of Ankylosauridae, Ceratopsidae, and Hadrosauridae, suggesting that detection probability significantly changes between temporal intervals. Covariate  $\beta$  estimates show similar patterns to the broader detection probabilities previously observed with the sparta model; Ankylosauridae and Hadrosauridae show increasingly reduced detection probability in later bins (e.g., Ankylosauridae, 0.5°, 10 max. visits: bin 4 [66.7 Ma]:  $\beta = -1.694$ ; 95% BCI = -2.785 to -0.593; Hadrosauridae,  $0.5^{\circ}$ , 40 max. visits:  $\beta = -0.849$ , 95% BCI = -1.34 to -0.36), whereas Ceratopsidae show the opposite (e.g.,  $0.5^{\circ}$ , 40 max. visits, bin 4 [66 Ma]:  $\beta = 1.006$ ; 95% BCI = 0.366-1.632). Higher modern rainfall negatively impacts the detection of Ankylosauridae and Hadrosauridae at 1° resolution when the maximum number of visits is capped at 10 (Ankylosauridae:  $\beta = -0.694$ ; 95% BCI = -1.574 to -0.02; Hadrosauridae:  $\beta = -0.299$ ; 95% BCI = -0.566 to -0.053). Increased distance from roads positively impacts the detection of Ceratopsidae within models using 40 maximum visits (0.5°:  $\beta = 0.196$ ; 95% BCI = 0.032 to 0.364; 1°:  $\beta$  = 0.221; 95% BCI = 0.074–0.378), whereas increased sediment flux shows a negative impact on their detection probability at 0.5° resolution (10 max. visits:  $\beta = -0.441$ ; 95% BCI = -0.734 to -0.146; 40 max. visits:  $\beta = -0.461$ ; 95% BCI = -0.787 to -0.142). The number of total collections and maximum green vegetation fraction are present in the best-fitting models of several families, but none have a



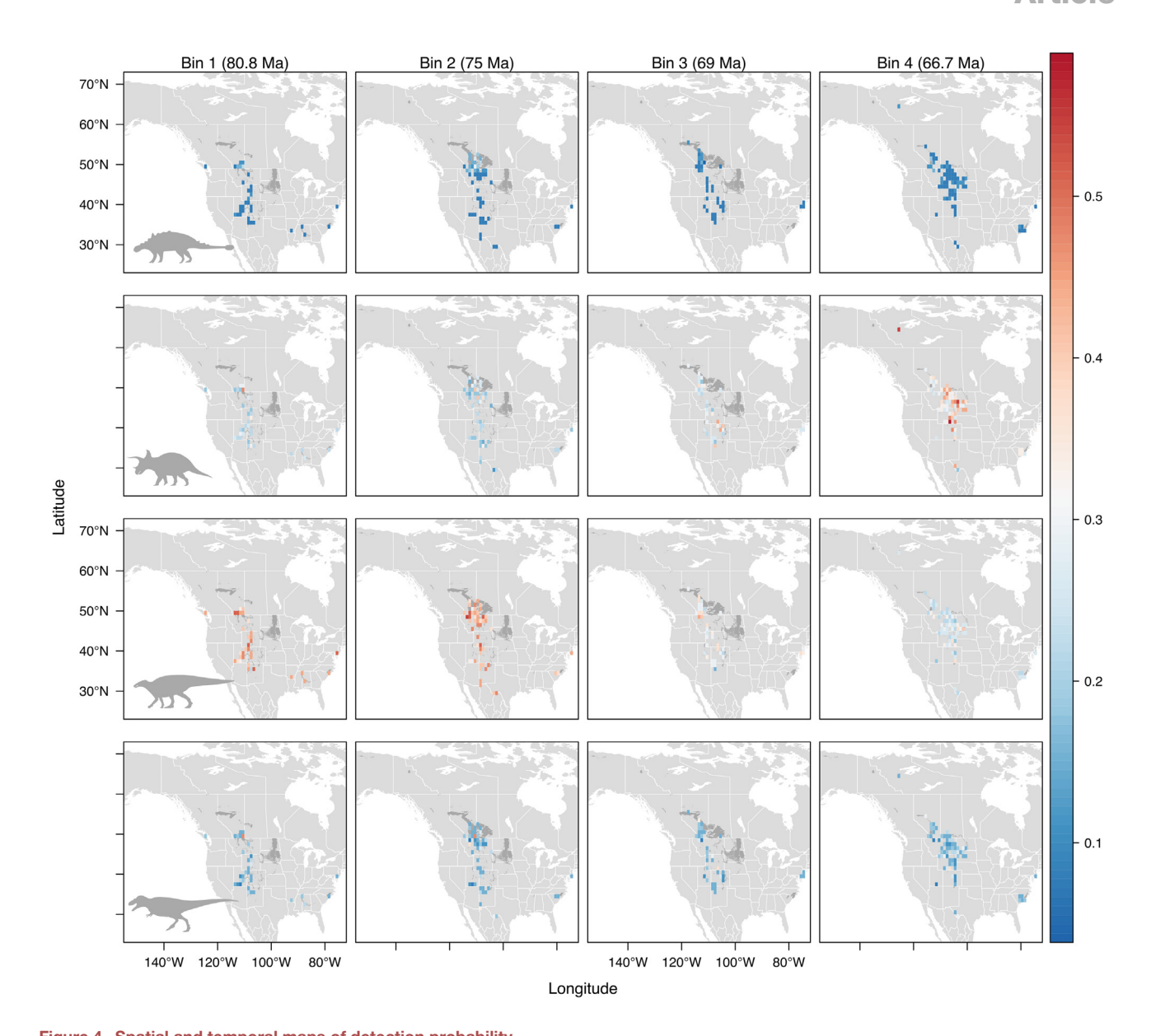


Figure 4. Spatial and temporal maps of detection probability

Maps showing average detection probability of dinosaur clades at a given site through time in North America, generated from best-fitting models of multi-season spatially explicit Bayesian models run using spOccupancy at 1° × 1° resolution and with the maximum number of visits capped at 40. Dark gray areas represent geological outcrop for the respective time bin. Ankylosauridae silhouette produced by Andrew Farke, 2013, CC BY 3.0; Hadrosauridae and Tyrannosauridae silhouettes produced by Matthew Dempsey, 2020, CC BY 3.0; Ceratopsidae silhouette produced by Ivan Iofrida, 2024, CC BY 4.0.

See also Figure S5 and Table S8.

significant effect. Several other non-significant covariates appearing in best-fitting models have moderate support for impacting detection probability due to BCI values overlapping 0 by a marginal amount and a high probability of the effect being greater than 0 (Ankylosauridae: distance from roads [0.5°, 10 max. visits], outcrop area [0.5°, 40 max. visits; 1°, 10 max. visits]; Ceratopsidae: time bins [0.5°, 10 max. visits; 1°, 10 and 40 max. visits]; Hadrosauridae: other land cover [1°, 10 max. visits]; see Table S2 for complete list). Additionally, all best-fitting models across clades feature the inclusion of a random effect varying by site, indicating unmodeled heterogeneity in detection probability across space (removal of this introduces goodness-of-fit

issues to the models) (Figure S5). It should also be noted that Tyrannosauridae report no statistically significant covariates in any of their best-fitting models and low probability of any effect size being greater than 0. Results are broadly consistent between different maximum numbers of visits, with magnitude and direction of covariate effects appearing similar (Figures 5 and 6).

For occupancy covariates, Ankylosauridae occupancy is significantly negatively affected by mean temperature of the hottest quarter (0.5°, 10 max. visits:  $\beta = -2.502$ ; 95% BCI = -4.499 to -0.428). Ceratopsidae occupancy is negatively affected by mean precipitation of the driest quarter at both spatial resolutions and numbers of maximum visits (10 max. visits, 0.5°:  $\beta = -1.24$ ;



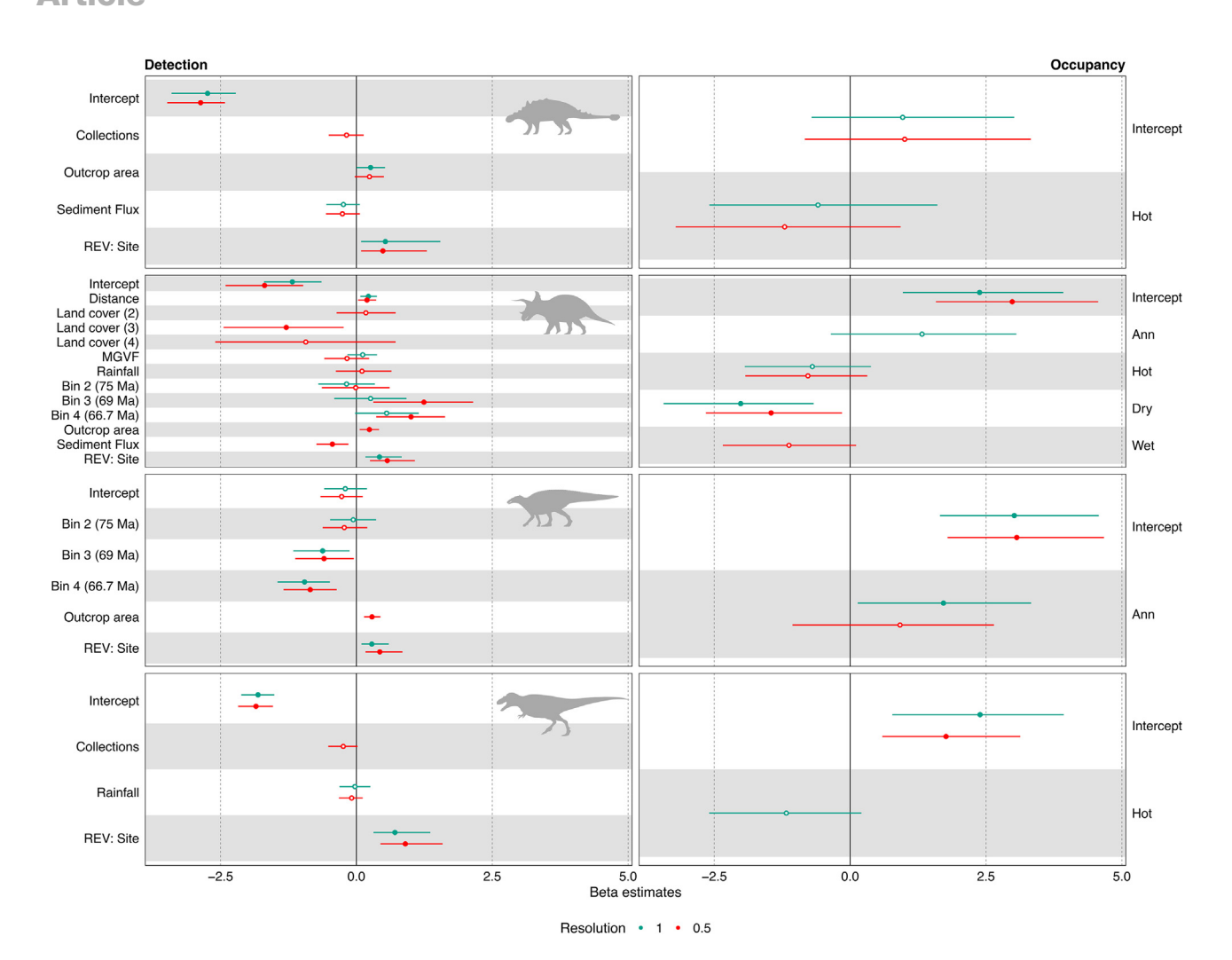


Figure 5. Occupancy and detection covariates for multi-season models (spOccupancy), maximum visits capped at 40

Forest plots of covariate beta estimates and associated BCIs (95%) from best-fitting models of multi-season spatially explicit Bayesian models run using spOccupancy at both 0.5° × 0.5° and 1° × 1° resolution, with maximum visits capped at 40. Covariates with solid fill indicate statistically significant results (BCIs do not cross 0). Left-hand side shows detection covariates, whereas the right-hand side reports occupancy covariates. Distance: distance to nearest road for each collection in the model. Land cover (2): open terrain. Land cover (3): forested terrain. Land cover (4): other. MGVF, maximum green vegetation fraction; REV, random effect variance. Ankylosauridae silhouette produced by Andrew Farke, 2013, CC BY 3.0; Hadrosauridae and Tyrannosauridae silhouettes produced by Matthew Dempsey, 2020, CC BY 3.0; Ceratopsidae silhouette produced by Ivan Iofrida, 2024, CC BY 4.0.

See also Figures S5 and S6 and Tables S1, S2, and S8.

95% BCI = -2.315 to -0.074.  $1^{\circ}$ :  $\beta$  = -1.684; 95% BCI = -3.177 to -0.438; 40 max. visits,  $0.5^{\circ}$ :  $\beta$  = -1.454; 95% BCI = -2.653 to -0.149,  $1^{\circ}$ :  $\beta$  = -2.013; 95% BCI = -3.431 to -0.671), as well as annual mean temperature standard deviation at  $1^{\circ}$  resolution and 10 maximum visits ( $\beta$  = 1.668; 95% BCI = 0.079-3.315). Hadrosauridae occupancy is positively affected by mean annual temperature standard deviation ( $1^{\circ}$ , 40 max. visits:  $\beta$  = 1.718; 95% BCI = 0.139-3.331). Only marginally significant coefficients are observed for Tyrannosauridae (negative effect; mean temperature of the hottest quarter).

#### **DISCUSSION**

Our results indicate that apparent declines in naive occupancy of dinosaur clades observed in the North American fossil record are a consequence of overall decreased detection probability in the Maastrichtian rather than genuine reductions in occupancy, indicating that mean occupancy probability either increased or remained stable up to the K/Pg boundary (Figures 2 and 3; supporting Figure 1B scenario 2). It is therefore our ability to detect dinosaur occurrences that appears to be the dominant control on their observable spatiotemporal distribution, rather than this reflecting a true biological signal. This provides evidence of the hypothesized shift in available sampling window between the Campanian and Maastrichtian, 18 indicating that our understanding of Maastrichtian dinosaurs is inhibited by the geological record. This finding is supported by examining the drivers of detection probability of dinosaur families through geological time. Although a variety of covariates contribute to driving patterns of dinosaur detection probability, increased outcrop area most consistently appears as a statistically significant driver across clades (Figures 5 and 6), and, when it is



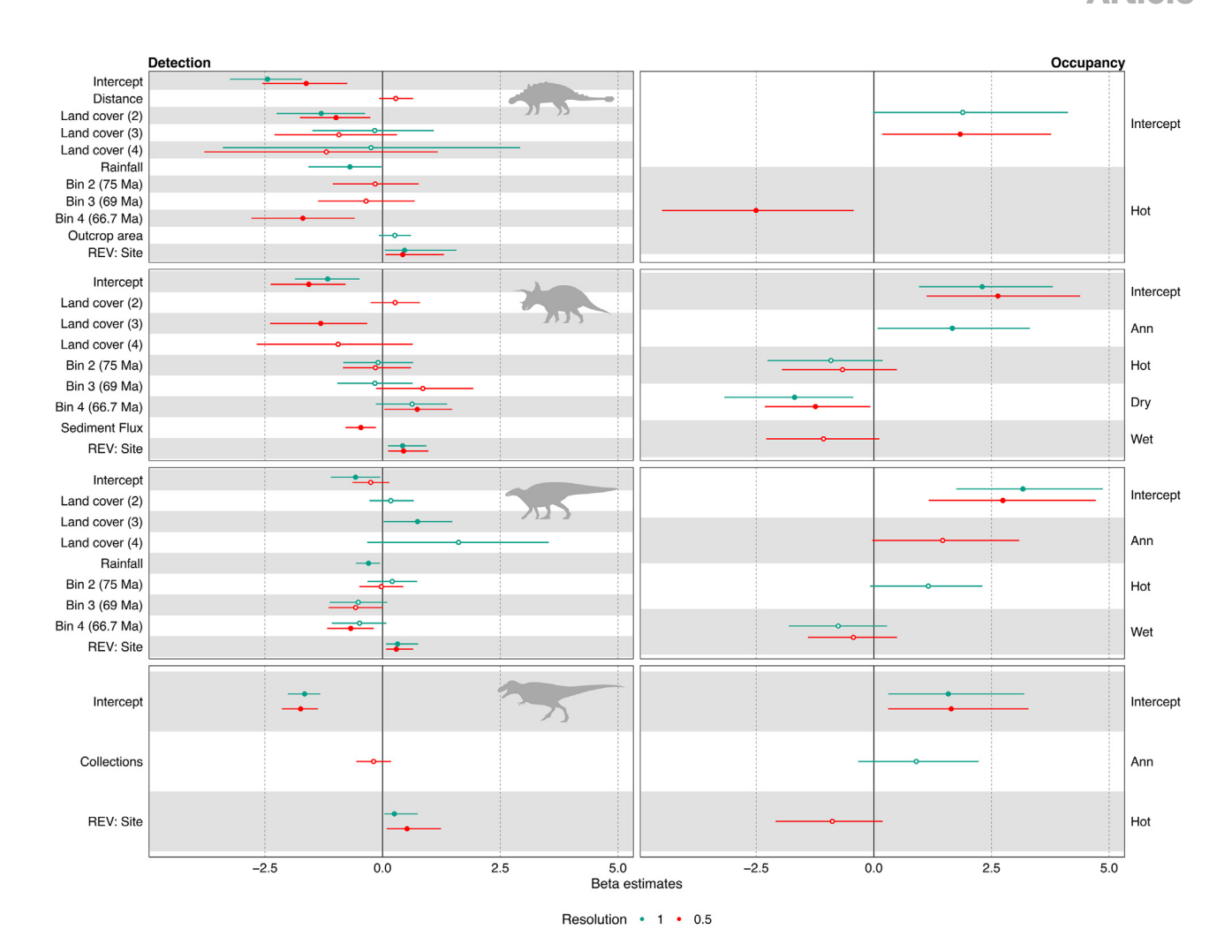


Figure 6. Occupancy and detection covariates for multi-season models (spOccupancy), maximum visits capped at 10

Forest plots of covariate beta estimates and associated BCIs (95%) from best-fitting models of multi-season spatially explicit Bayesian models run using spOccupancy at both 0.5° × 0.5° and 1° × 1° resolution, with maximum visits capped at 10. Covariates with solid fill indicate statistically significant results (BCIs do not cross 0). Left-hand side shows detection covariates, whereas the right-hand side reports occupancy covariates. Distance: distance to nearest road for each collection in the model. Land cover (2): open terrain. Land cover (3): forested terrain. Land cover (4): other. MGVF, maximum green vegetation fraction; REV, random effect variance. Ankylosauridae silhouette produced by Andrew Farke, 2013, CC BY 3.0; Hadrosauridae and Tyrannosauridae silhouettes produced by Matthew Dempsey, 2020, CC BY 3.0; Ceratopsidae silhouette produced by Ivan Iofrida, 2024, CC BY 4.0.

See also Figures S5 and S6 and Tables S1, S2, and S8.

missing from the best-fitting model, it consistently appears as a covariate in at least one of the top three models with the lowest widely applicable information criterion (WAIC) (see supplemental information, results folder). Geological outcrop area in North America has been reported to show a close relationship with dinosaur diversity through time, <sup>18,71</sup> but previous studies have failed to find a direct impact of outcrop on the spatial distribution of dinosaurs within the WIB. <sup>24</sup> By intrinsically incorporating spatial sampling heterogeneity, our models suggest that outcrop availability has a direct and statistically significant impact on the sampling of North American dinosaurs prior to their extinction.

As counts of sampling proxies (e.g., the number of collections or the number of dinosaur-bearing formations) are approximately equally high during the Campanian and the Maastrichtian, the North American fossil record has been viewed as containing a

relatively accurate reflection of dinosaur dynamics in the lead-up to the K/Pg boundary. Similarly, Condamine et al. 10 found that estimates of mean preservation rates of dinosaur occurrences calculated using PyRate showed an increase between the Campanian and the Maastrichtian, implying that the fossil record could likely be fairly compared between the two time intervals. However, our results indicate that the intensity of sampling is not a dominant control on the detection of dinosaur clades within the latest Cretaceous. The probability of detecting an occurrence of the four clades in the present work does not follow the trajectory of previous studies; only Ceratopsidae shows an unambiguous increase in detection probability through the latest Cretaceous (Figures 2 and 3), likely due to the relative overabundance of the taxon *Triceratops* in the Lancian. Despite including the number of collections as a potential covariate during model



Res.	Max. value	Target	Occupancy formula	Detection formula	elpd	pD	WsAIC
0.5	10	Ankylosauridae	hot	land cover (2) + land cover (3) + land cover (4) + distance + bin 2 (75 Ma) + bin 3 (69 Ma) + bin 4 (66.7 Ma)	-181.78	19.39	402.33
0.5	10	Ceratopsidae	wet + dry + hot	sediment flux + land cover (2) + land cover (3) + land cover (4) + bin 2 (75 Ma) + bin 3 (69 Ma) + bin 4 (66.7 Ma)	-466.42	47.35	1,027.55
0.5	10	Hadrosauridae	wet + Ann.	bin 2 (75 Ma) + bin 3 (69 Ma) + bin 4 (66.7 Ma)	-581.02	42.91	1,247.87
0.5	10	Tyrannosauridae	hot	collections	-344.46	37.39	763.69
1	10	Ankylosauridae	~1	outcrop area + rainfall + land cover (2) + land cover (3) + land cover (4)	-143.70	14.16	315.71
1	10	Ceratopsidae	dry + hot + Ann	bin 2 (75 Ma) + bin 3 (69 Ma) + bin 4 (66.7 Ma)	-364.51	33.99	797.00
1	10	Hadrosauridae	wet + hot	rainfall + land cover (2) + land cover (3) + land cover (4) + bin 2 (75 Ma) + bin 3 (69 Ma) + bin 4 (66.7 Ma)	-444.52	40.05	969.15
1	10	Tyrannosauridae	Ann.	~1	-279.11	18.95	596.11
0.5	40	Ankylosauridae	hot	outcrop area + sediment flux + collections	-293.32	23.00	632.63
0.5	40	Ceratopsidae	wet + dry + hot	outcrop area + sediment flux + MGVF + rainfall + land cover (2) + land cover (3) + land cover (4) + distance + bin 2 (75 Ma) + bin 3 (69 Ma) + bin 4 (66.7 Ma)	-838.19	57.45	1,791.28
0.5	40	Hadrosauridae	Ann.	outcrop area + bin 2 (75 Ma) + bin 3 (69 Ma) + bin 4 (66.7 Ma)	-989.25	62.65	2,103.79
0.5	40	Tyrannosauridae	~1	rainfall + collections	-603.87	49.86	1,307.46
1	40	Ankylosauridae	hot	outcrop area + sediment flux	-265.86	21.23	574.18
1	40	Ceratopsidae	dry + hot + Ann.	MGVF + distance + bin 2 (75 Ma) + bin 3 (69 Ma) + bin 4 (66.7 Ma)	-706.82	43.98	1,501.59
1	40	Hadrosauridae	Ann.	bin 2 (75 Ma) + bin 3 (69 Ma) + bin 4 (66.7 Ma)	-835.15	46.18	1,762.66
1	40	Tyrannosauridae	hot	rainfall	-515.15	38.72	1,107.73

Table showing the best-fitting models for each clade, at each spatial resolution and maximum number of visits, for multi-season occupancy models run using spOccupancy. Res., resolution; Max. value, maximum number of collections used for each site; elpd, expected log point-wise predictive density; pD, effective number of parameters; WAIC, widely applicable information criterion; Ann., mean annual temperature standard deviation; land cover (2), open terrain; land cover (3), forested terrain; land cover (4), other; MGVF, maximum green vegetation fraction. See Tables S1, S2, and S8.

selection, this variable fails to appear as a statistically significant component of any best-fitting model (Figures 5 and 6). Furthermore, models run using a cap of 10 versus 40 maximum visits (i.e., collections herein) per site show no significant difference in the trajectory of detection probability through time or in the magnitude of covariates within the best-fitting models for all clades. Capping the maximum number of visits per site within the occupancy modeling framework aims to reduce the possibility of preferential sampling at specific locations having an impact on the estimated values of detection covariates <sup>73</sup> (e.g., a site with 80 visits will have a comparatively larger impact on the estimated values of detection covariates than sites with only 2 or 3 visits).

Broad consistency across our results therefore indicates that sites with particularly high numbers of collections are not significantly impacting estimates of detection probability. It is therefore the spatial arrangement of data that is primarily driving estimates of detection probability through time, supporting the hypothesis that changes in the spatiotemporal sampling window have impacted the detectability and recovery of dinosaur clades within the Maastrichtian. Combined, these factors show that it is not just the intensity of sampling (e.g., the total number of fossiliferous collections) that impacts our understanding of past macroecological patterns but also the physical constraints that the geological record imposes on that sample.



These results have knock-on implications for the ongoing debate on whether non-avian dinosaurs were in decline prior to their extinction at the K/Pg boundary. Allen et al. 15 found that assumptions regarding sampling strongly impacted estimates of diversification rates when using phylodynamic models and concluded that accurately modeling sampling biases is key to resolving this issue. Our results align with Allen et al. 15 in suggesting that the discrepancy of sampling within the latest Cretaceous intrinsically hinders efforts to establish whether non-avian dinosaurs were in decline. It is possible that overall poor detection probability could reduce the number of species we are able to sample from the Maastrichtian, particularly for Hadrosauridae, and thus deflate overall diversity estimates for these clades during this interval; but, given that our estimates are taken at the family level and do not directly estimate species richness, this is not something our study has the power to resolve. However, quantifying detection probability through time fulfills the goal of more accurately modeling sampling biases and can facilitate other approaches to produce realistic estimates of diversity within the latest Cretaceous. DeepDive, a new diversity estimation approach, uses a combination of mechanistic simulations and deep learning to infer species richness while accounting for spatial, temporal, and taxonomic variation in sampling.<sup>7</sup> This approach requires inputs regarding the likelihood of clades being sampled through both space and time<sup>74</sup>; estimates of detectability included here could help inform such studies. providing realistic estimates and associated confidence intervals for the sampling of specific clades.

Our work also clarifies arguments about the distribution of dinosaurs within the Maastrichtian. Applying ecological niche modeling, Chiarenza et al. 18 reported consistent habitat suitability for dinosaurs in North America throughout the latest Cretaceous, suggesting that long-term climatic shifts did not influence their extinction. However, ecological niche modeling, by definition, only identifies the potential areas that a taxon may inhabit rather than their genuine biogeographic occupancy. 75 As such, although suitable habitat area may have remained stable - or even shown a Campanian-to-Maastrichtian increase - it has been argued that these areas may not necessarily have been inhabited by high numbers of dinosaur taxa due to historical, biogeographic, or biotic constraints.<sup>75</sup> By accounting for imperfect detection, we show that the mean occupancy probability of North American dinosaurs remained stable up until the K/Pg boundary, broadly tracking the available suitable habitat area for these clades. 18 Furthermore, occupancy—and, more broadly, geographical distribution-is widely regarded as a strong predictor of extinction risk within both modern and ancient ecosystems, with low geographic occupancy resulting in higher rates of extinction. 60,76-79 Stable or increasing occupancy trajectories for the dinosaur families studied here suggest that populations were widespread and successful throughout the latest Cretaceous, at least in North America, and therefore unlikely to be at direct risk of extinction due to a restricted range prior to bolide impact at the K/Pg boundary. Changes in detectability through time also provide additional context for the interpretation of macroevolutionary patterns. It is possible that reduced detectability for Hadrosauridae in the Maastrichtian could impact our ability to discover new species for this clade, resulting in reduced apparent diversity prior to the K/Pg boundary. Conversely, detection probability of Ceratopsidae increases toward the end-Maastrichtian, despite the clade experiencing the strongest overall diversification decline out of the major dinosaur clades in the study of Condamine et al., <sup>10</sup> which might be interpreted as support for genuinely lower ceratopsid diversity at the end-Cretaceous. Although our results do not directly address changes in diversity, the combination of agents discussed above indicates that the North American fossil record of dinosaurs in the Maastrichtian is negatively influenced by sampling biases, and, thus, diversity of the clade is potentially higher than has been previously estimated. However, it should also be noted that these findings can only be considered confidently in light of the North American fossil record and global patterns are likely to be regionally heterogeneous. <sup>47</sup>

Although our results allow for interpretation of the relative importance of associated covariates, other underlying drivers for changes in sampling between the Campanian and Maastrichtian<sup>18</sup> are less clear. Clades exhibiting simultaneous declines in detection probability show no common explanatory environmental drivers. Furthermore, removing occurrences of smallbodied taxa (Mammalia, Squamata, and Amphibia) produced no significant variation in results (Figure S6), indicating that an increased proportion of vertebrate microsites within the Maastrichtian is having no impact on large-bodied taxa showing reduced detection probability prior to the K/Pg boundary. However, all models report relatively high values for random effects varying by site and show poor goodness-of-fit without their inclusion, indicating a degree of unmodeled heterogeneity in detection probability across space that is not accounted for by present model covariates (Figures 5 and 6; Figure S5). Heterogeneity in detection probability often occurs in occupancy models because of substantial variation in the abundance of the target taxon between sites due to the increased probability of detecting the taxon when there are more individuals to detect.<sup>80</sup> As such, there is a possibility that this unmodeled heterogeneity in detection probability is a result of local variation in fossil preservation rate between sites. Although we chose a wide range of covariates to cover potential sources of bias, the majority are regionally scaled and attributed to sites (grid cells), rather than visits (collections), within the occupancy framework, which by necessity have relatively coarse spatial resolutions and may be an abstraction from the intended sampling impacts. This is an indication that geological factors at the locality or collection level are likely to exert a strong additional control on preservation rate and subsequently fossil recovery that is not covered by these more regional proxies. These results show that the detectability of organisms in deep time is complex, with multiple drivers at both the local and continental scales. Future efforts to evaluate spatial biases in the fossil record should aim to incorporate collections-level geological information alongside regional environmental datasets.

The differences in detection probability trajectories between families may indicate other taphonomic processes that control our understanding of North American dinosaurs. Hadrosauridae and Ceratopsidae show opposing trajectories of detection probability during the Maastrichtian, despite being megaherbivorous lineages with similar preservation potentials. This difference may reflect habitat preference; several authors have shown that Ceratopsidae and Hadrosauridae show differential associations





with specific lithologies and environments within the Cretaceous. Lyson and Longrich<sup>83</sup> showed preferential preservation of Ceratopsidae and Hadrosauridae within mudstones and sandstones, respectively, in the Maastrichtian of North America, which they inferred to be spatial niche partitioning between floodplain and fluvial environments (although see Mallon<sup>84</sup>). Similarly, Butler and Barrett85 found statistical support for Hadrosauridae to be associated with marine sediments and marginocephalians with terrestrial deposits. Contrast in detection probability trajectory could therefore represent a change in the broadscale proportion of exposed sandstones to mudstones during the Maastrichtian, potentially as a result of the retreat of the WIS and combined reduced sediment fluxes and enhanced erosivity. 18 This is also potentially supported by Ceratopsidae detection probability showing a negative impact from increased sediment flux at 0.5° × 0.5° resolution (Figures 5 and 6), which is not seen in Hadrosauridae. Hadrosauridae also shows the highest overall detection probability, as well as proportionally increased detection in collections, with fewer genera compared with the other lineages examined (Figures 2 and S4). This could be an indication of high abundance of hadrosaurids within latest Cretaceous ecosystems and/or that their remains are more easily identifiable and recoverable than those of Ceratopsidae and Tyrannosauridae. Detection probability is low within all model results for Ankylosauridae and Tyrannosauridae, which is likely due to data quality; these clades have the lowest number of occurrences out of the four families examined and low overall detections within the occupancy model (e.g., out of 1,601 visits to sites within sparta model, run at 0.5° × 0.5°, Ankylosauridae report 108 detections and Tyrannosauridae report 166). Although occupancy modeling has obvious applicability in palaeontology, 61,62,64,65 it is a "data-hungry" technique, and, thus, consideration should be taken for the study system and target taxon when applied to other areas of the fossil record. Occupancy modeling may not be an appropriate technique for clades and systems where data, both in terms of fossils and covariates, are particularly sparse.

Occupancy modeling using paleontological occurrence data is subject to the same limitations as neontological studies using similar presence-only datasets to assess trends in occupancy and detection probability through time. Reducing the spatial and/or temporal resolution of sparse ecological data to enhance model performance and precision is common practice in occupancy modeling.<sup>69</sup> Our results align with Jönsson et al.,<sup>69</sup> indicating that coarsening the spatiotemporal resolution has minimal impact on overall occupancy trends or model performance with sparsely collected data and underscores the suitability of occupancy modeling for opportunistically gathered paleontological datasets.

Comprehending and constraining the impact of fossil record biases is crucial for understanding past life, and it is now increasingly seen as a critical step for studies using the fossil record to provide context and baselines for modern conservation efforts.86 Spatial data absence and sampling heterogeneity have been singled out as major contributors to fossil record bias, making them a significant barrier to interrogating macroecological patterns in both deep and shallow time. 10,32,34,43,46,48,87 Here, we show that by providing spatially explicit probabilistic estimates of both occupation and detection, occupancy modeling contributes to understanding the complex interplay between spatial heterogeneity and the underlying structure of the fossil record. This ability to quantify imperfect detection and recognize true absence within a spatial framework can facilitate an understanding of the "architecture" of the fossil record<sup>88</sup>—i.e., how and why fossil record quality changes through both time and space - which is, in turn, essential for drawing accurate comparison between, and realistic conclusions about, organisms and events in the deep past. Understanding the probable distribution of taxa across space while accounting for absent data additionally has potential in the field of conservation paleobiology, which seeks to establish baselines in species occupancy through time.86 Comparatively abundant Holocene records89 will also combat the data-hungry nature of occupancy modeling. Our results demonstrate that occupancy models can be integrated with occurrence-based records from large, opportunistically collected datasets to extract meaningful information from the relatively sparse vertebrate fossil record.

#### RESOURCE AVAILABILITY

#### **Lead contact**

Further information and requests for resources should be directed to and will be fulfilled by the lead contact, Christopher D. Dean (christopher.dean@ucl.ac.uk).

#### **Materials availability**

This study did not generate unique materials.

#### Data and code availability

All fossil occurrence data, original code, and raw results used in this study have been deposited at Zenodo and are publicly available as of the date of publication at https://doi.org/10.5281/zenodo.14946419.

R scripts are also available at https://github.com/ChristopherDavidDean/ NA-Dino-Occ.

Any additional information required to reanalyze the data reported in this paper is available from the lead contact upon request.

#### **ACKNOWLEDGMENTS**

This work greatly benefited from discussions with the Palaeobiology Group at the University of Birmingham, UK. We are grateful to Maria Victoria Jimenez Franco, who provided assistance with a preliminary version of the project, to Christopher Scotese for his assistance with paleogeographies, and to Nick Isaac for assistance with posterior prediction checks and for providing code. We would also like to thank Andrew Farke, Ivan Iofrida, and Matthew Dempsey for silhouette illustrations obtained from Phylopic, as well as all enterers of data in the Paleobiology Database. This manuscript was greatly improved by insightful and constructive comments from four anonymous reviewers, as well as editorial assistance by Florian Maderspacher. We also thank three anonymous reviewers for constructive comments on a previous version of this manuscript. C.D.D. would also like to thank Therese Donovan, Alexej Siren, and Jim Hines for providing knowledge and expertise on occupancy modeling and Megan Renoir for assistance with manuscript edits. C.D.D. was supported by a Royal Society grant (RF\_ERE\_210013, awarded to P.D.M.), as well as by the European Union's Horizon 2020 research and innovation programme under grant no. 637483 (ERC Starting Grant TERRA was awarded to R.J.B.). A.A.C. was supported through the European Research Council (ERC) starting grant under the European Union's Horizon 2020 research and innovation program, grant agreement no. 947921 and MAPAS at the Universidade de Vigo (Spain). A.A.C. was also supported by a Juan de la Cierva-formación 2020 fellowship funded by FJC2020-044836-I/MCIN/ AEI/10.13039/501100011033 through the European Union "NextGenerationEU"/PRTR and by a Royal Society Newton International Fellowship (NIF\R1\231802), A.F. acknowledges Chinese Academy of Sciences Visiting Professorship for Senior International Scientists 2021FSE0001 and NERC





grants NE/V011405/1, NE/X000222/1, and NE/X015505/1. L.A.J. was supported by a Juan de la Cierva-formación 2021 fellowship (FJC2021-046695-1) funded by MCIN/AEI/10.13039/501100011033 and the European Union NextGenerationEU/PRTR, as well as a NERC Independent Research Fellowship (UKRI185). P.D.M.'s contribution was supported by grants from The Royal Society (UF160216, RGF\R1\180020, RGF\EA\201037, and URF\_R\_221010). This is Paleobiology Database official publication number 520.

#### **AUTHOR CONTRIBUTIONS**

Conceptualization, C.D.D.; methodology, C.D.D.; software: C.D.D. and L.A.J.; formal analysis: C.D.D., J.W.D., A.F., S.J.L., and C.L.O.; investigation: C.D.D., A.A.C., J.W.D., L.A.J., and P.D.M.; resources: A.A.C., A.F., J.W.D., L.A.J., S.J.L., C.L.O., P.J.V., and P.D.M.; data curation: C.D.D.; writing – original draft: C.D.D.; writing – review & editing: C.D.D., A.A.C., J.W.D., A.F., L.A.J., S.J.L., C.L.O., R.J.B., and P.D.M.; visualization: C.D.D.; supervision: R.J.B. and P.D.M.; project administration: C.D.D.; funding acquisition: R.J.B. and P.D.M.

#### **DECLARATION OF INTERESTS**

The authors declare no competing interests.

#### **STAR**\*METHODS

Detailed methods are provided in the online version of this paper and include the following:

- KEY RESOURCES TABLE
- METHOD DETAILS
  - Occurrence dataset and data preparation
  - o Temporal and spatial resolution
  - Model covariates
- QUANTIFICATION AND STATISTICAL ANALYSIS
  - Occupancy modelling

#### SUPPLEMENTAL INFORMATION

Supplemental information can be found online at https://doi.org/10.1016/j.cub.2025.03.025.

Received: September 6, 2024 Revised: February 11, 2025 Accepted: March 13, 2025 Published: April 8, 2025

#### REFERENCES

- Schulte, P., Alegret, L., Arenillas, I., Arz, J.A., Barton, P.J., Bown, P.R., Bralower, T.J., Christeson, G.L., Claeys, P., Cockell, C.S., et al. (2010). The Chicxulub Asteroid Impact and Mass Extinction at the Cretaceous-Paleogene Boundary. Science 327, 1214–1218. https://doi.org/10. 1126/science.1177265.
- Chiarenza, A.A., Farnsworth, A., Mannion, P.D., Lunt, D.J., Valdes, P.J., Morgan, J.V., and Allison, P.A. (2020). Asteroid impact, not volcanism, caused the end-Cretaceous dinosaur extinction. Proc. Natl. Acad. Sci. USA 117, 17084–17093. https://doi.org/10.1073/pnas.2006087117.
- Field, D.J., Bercovici, A., Berv, J.S., Dunn, R., Fastovsky, D.E., Lyson, T.R., Vajda, V., and Gauthier, J.A. (2018). Early evolution of modern birds structured by global forest collapse at the end-Cretaceous mass extinction. Curr. Biol. 28, 1825–1831.e2. https://doi.org/10.1016/j.cub.2018. 04.062.
- Smith, F.A., Boyer, A.G., Brown, J.H., Costa, D.P., Dayan, T., Ernest, S.K.M., Evans, A.R., Fortelius, M., Gittleman, J.L., Hamilton, M.J., et al. (2010). The Evolution of Maximum Body Size of Terrestrial Mammals. Science 330, 1216–1219. https://doi.org/10.1126/science.1194830.

- Sakamoto, M., Benton, M.J., and Venditti, C. (2016). Dinosaurs in decline tens of millions of years before their final extinction. Proc. Natl. Acad. Sci. USA 113, 5036–5040. https://doi.org/10.1073/pnas.1521478113.
- Bonsor, J.A., Barrett, P.M., Raven, T.J., and Cooper, N. (2020). Dinosaur diversification rates were not in decline prior to the K-Pg boundary. R. Soc. Open Sci. 7, 201195. https://doi.org/10.1098/rsos.201195.
- Sakamoto, M., Benton, M.J., and Venditti, C. (2021). Strong support for a heterogeneous speciation decline model in Dinosauria: a response to claims made by Bonsor et al. (2020). R. Soc. Open Sci. 8, 202143. https://doi.org/10.1098/rsos.202143.
- Sakamoto, M., Benton, M., and Venditti, C. (2021). Diversification Declines in Major Dinosaurian Clades are not Because of Edge Effects or Incomplete Fossil Sampling. Preprint at Research Square.
- Han, F., Wang, Q., Wang, H., Zhu, X., Zhou, X., Wang, Z., Fang, K., Stidham, T.A., Wang, W., Wang, X., et al. (2022). Low dinosaur biodiversity in central China 2 million years prior to the end-Cretaceous mass extinction. Proc. Natl. Acad. Sci. USA 119, e2211234119. https://doi. org/10.1073/pnas.2211234119.
- Condamine, F.L., Guinot, G., Benton, M.J., and Currie, P.J. (2021).
   Dinosaur biodiversity declined well before the asteroid impact, influenced by ecological and environmental pressures. Nat. Commun. 12, 3833. https://doi.org/10.1038/s41467-021-23754-0.
- Fastovsky, D.E., Huang, Y., Hsu, J., Martin-McNaughton, J., Sheehan, P.M., and Weishampel, D.B. (2004). Shape of Mesozoic dinosaur richness. Geology 32, 877–880. https://doi.org/10.1130/G20695.1.
- Sarjeant, W.A.S., and Currie, P.J. (2001). The "Great Extinction" that never happened: the demise of the dinosaurs considered. Can. J. Earth Sci. 38, 239–247. https://doi.org/10.1139/e00-077.
- Brusatte, S.L., Butler, R.J., Prieto-Márquez, A., and Norell, M.A. (2012).
   Dinosaur morphological diversity and the end-Cretaceous extinction.
   Nat. Commun. 3, 804. https://doi.org/10.1038/ncomms1815.
- Brusatte, S.L., Butler, R.J., Barrett, P.M., Carrano, M.T., Evans, D.C., Lloyd, G.T., Mannion, P.D., Norell, M.A., Peppe, D.J., Upchurch, P., et al. (2015). The extinction of the dinosaurs. Biol. Rev. Camb. Philos. Soc. 90, 628–642. https://doi.org/10.1111/brv.12128.
- Allen, B.J., Volkova Oliveira, M.V., Stadler, T., Vaughan, T.G., and Warnock, R.C.M. (2024). Mechanistic phylodynamic models do not provide conclusive evidence that non-avian dinosaurs were in decline before their final extinction. Camb. Prism Extinct 2, e6. https://doi.org/10.1017/ ext.2024.5.
- Fastovsky, D.E., and Sheehan, P.M. (2005). The extinction of the dinosaurs in North America. GSA Today 15, 4–10. https://doi.org/10.1130/1052-5173(2005)15<4:TEOTDI>2.0.CO;2.
- Archibald, J.D. (2014). What the dinosaur record says about extinction scenarios. Geol. Soc. Am. Spec. Pap. 505, 213–224.
- Chiarenza, A.A., Mannion, P.D., Lunt, D.J., Farnsworth, A., Jones, L.A., Kelland, S.-J., and Allison, P.A. (2019). Ecological niche modelling does not support climatically-driven dinosaur diversity decline before the Cretaceous/Paleogene mass extinction. Nat. Commun. 10, 1091. https://doi.org/10.1038/s41467-019-08997-2.
- Dean, C.D., Chiarenza, A.A., and Maidment, S.C.R. (2020). Formation binning: a new method for increased temporal resolution in regional studies, applied to the Late Cretaceous dinosaur fossil record of North America. Palaeontology 63, 881–901. https://doi.org/10.1111/pala. 12492.
- Roberts, E.M., Deino, A.L., and Chan, M.A. (2005). 40Ar/39Ar age of the Kaiparowits Formation, southern Utah, and correlation of contemporaneous Campanian strata and vertebrate faunas along the margin of the Western Interior Basin. Cret. Res. 26, 307–318. https://doi.org/10. 1016/j.cretres.2005.01.002.
- Gates, T.A., Sampson, S.D., Zanno, L.E., Roberts, E.M., Eaton, J.G., Nydam, R.L., Hutchison, J.H., Smith, J.A., Loewen, M.A., and Getty, M.A. (2010). Biogeography of terrestrial and freshwater vertebrates from the Late Cretaceous (Campanian) Western Interior of North

#### **Article**



- America. Palaeogeogr. Palaeoclimatol. Palaeoecol. 291, 371–387. https://doi.org/10.1016/i.palaeo.2010.03.008.
- Fowler, D.W. (2017). Revised geochronology, correlation, and dinosaur stratigraphic ranges of the Santonian-Maastrichtian (Late Cretaceous) formations of the Western Interior of North America. PLoS One 12, e0188426. https://doi.org/10.1371/journal.pone.0188426.
- Chiarenza, A.A., and Brusatte, S.L. (2023). Dinosaurs, Extinction Theories for. In Reference Module in Life Sciences (Elsevier). https://doi.org/10. 1016/B978-0-12-822562-2.00108-0.
- Maidment, S.C.R., Dean, C.D., Mansergh, R.I., and Butler, R.J. (2021).
   Deep-time biodiversity patterns and the dinosaurian fossil record of the Late Cretaceous Western Interior, North America. Proc. Biol. Sci. 288, 20210692. https://doi.org/10.1098/rspb.2021.0692.
- Russell, D.A. (1984). The gradual decline of the dinosaurs—fact or fallacy? Nature 307, 360–361. https://doi.org/10.1038/307360a0.
- Sheehan, P.M., Fastovsky, D.E., Hoffmann, R.G., Berghaus, C.B., and Gabriel, D.L. (1991). Sudden extinction of the dinosaurs: latest Cretaceous, upper Great Plains, USA. Science 254, 835–839. https:// doi.org/10.1126/science.11536489.
- Archibald, J.D., and Fastovsky, D.E. (2004). Dinosaur extinction. In The Dinosauria, 2 (University of California Press), pp. 672–684.
- Le Loeuff, J. (2012). Paleobiogeography and biodiversity of Late Maastrichtian dinosaurs: how many dinosaur species went extinct at the Cretaceous-Tertiary boundary? Bull. Soc. Geol. Fr. 183, 547–559. https://doi.org/10.2113/gssgfbull.183.6.547.
- Mannion, P.D. (2024). The spatiotemporal distribution of Mesozoic dinosaur diversity. Biol. Lett. 20, 20240443. https://doi.org/10.1098/rsbl. 2024.0443.
- Raup, D.M. (1972). Taxonomic diversity during the Phanerozoic. Science 177, 1065–1071. https://doi.org/10.1126/science.177.4054.1065.
- Alroy, J., Marshall, C.R., Bambach, R.K., Bezusko, K., Foote, M., Fürsich, F.T., Hansen, T.A., Holland, S.M., Ivany, L.C., Jablonski, D., et al. (2001). Effects of sampling standardization on estimates of Phanerozoic marine diversification. Proc. Natl. Acad. Sci. USA 98, 6261–6266. https://doi. org/10.1073/pnas.111144698.
- Benson, R.B.J., Butler, R., Close, R.A., Saupe, E., and Rabosky, D.L. (2021). Biodiversity across space and time in the fossil record. Curr. Biol. 31, R1225–R1236. https://doi.org/10.1016/j.cub.2021.07.071.
- Smith, A.B. (2001). Large–scale heterogeneity of the fossil record: implications for Phanerozoic biodiversity studies. Philos. Trans. R. Soc. Lond. B Biol. Sci. 356, 351–367. https://doi.org/10.1098/rstb.2000.0768.
- Close, R.A., Benson, R.B.J., Saupe, E.E., Clapham, M.E., and Butler, R.J. (2020). The spatial structure of Phanerozoic marine animal diversity. Science 368, 420–424. https://doi.org/10.1126/science.aay8309.
- Ye, S. (2024). Investigating the Role of Contemporary Climate on Fossil Collecting Bias. Paleontological Research 28, 413–425. https://doi.org/ 10.2517/PR230019.
- 37. Raja, N.B., Dunne, E.M., Matiwane, A., Khan, T.M., Nätscher, P.S., Ghilardi, A.M., and Chattopadhyay, D. (2022). Colonial history and global economics distort our understanding of deep-time biodiversity. Nat. Ecol. Evol. 6, 145–154. https://doi.org/10.1038/s41559-021-01608-8.
- Foote, M. (2001). Inferring temporal patterns of preservation, origination, and extinction from taxonomic survivorship analysis. Paleobiology 27, 602–630. https://doi.org/10.1666/0094-8373(2001)027<0602:ITPOPO> 2.0.CO:2.
- Walker, F.M., Dunhill, A.M., and Benton, M.J. (2020). Variable preservation potential and richness in the fossil record of vertebrates. Palaeontology 63, 313–329. https://doi.org/10.1111/pala.12458.

- Shaw, J.O., Briggs, D.E.G., and Hull, P.M. (2021). Fossilization potential of marine assemblages and environments. Geology 49, 258–262. https:// doi.org/10.1130/G47907.1.
- Foote, M., and Sepkoski, J.J., Jr. (1999). Absolute measures of the completeness of the fossil record. Nature 398, 415–417. https://doi. org/10.1038/18872.
- Vilhena, D.A., and Smith, A.B. (2013). Spatial bias in the marine fossil record. PLoS One 8, e74470. https://doi.org/10.1371/journal.pone. 0074470
- Benson, R.B.J., Butler, R.J., Alroy, J., Mannion, P.D., Carrano, M.T., and Lloyd, G.T. (2016). Near-stasis in the long-term diversification of Mesozoic tetrapods. PLoS Biol. 14, e1002359. https://doi.org/10.1371/journal.pbio.1002359.
- Close, R.A., Benson, R.B.J., Upchurch, P., and Butler, R.J. (2017).
   Controlling for the species-area effect supports constrained long-term Mesozoic terrestrial vertebrate diversification. Nat. Commun. 8, 15381. https://doi.org/10.1038/ncomms15381.
- Close, R.A., Benson, R.B.J., Alroy, J., Behrensmeyer, A.K., Benito, J., Carrano, M.T., Cleary, T.J., Dunne, E.M., Mannion, P.D., Uhen, M.D., et al. (2019). Diversity dynamics of phanerozoic terrestrial tetrapods at the local-community scale. Nat. Ecol. Evol. 3, 590–597. https://doi.org/ 10.1038/s41559-019-0811-8.
- Close, R.A., Benson, R.B.J., Alroy, J., Carrano, M.T., Cleary, T.J., Dunne, E.M., Mannion, P.D., Uhen, M.D., and Butler, R.J. (2020). The apparent exponential radiation of Phanerozoic land vertebrates is an artefact of spatial sampling biases. Proc. Biol. Sci. 287, 20200372. https://doi.org/ 10.1098/rspb.2020.0372.
- Flannery-Sutherland, J.T., Silvestro, D., and Benton, M.J. (2022). Global diversity dynamics in the fossil record are regionally heterogeneous. Nat. Commun. 13, 2751. https://doi.org/10.1038/s41467-022-30507-0.
- Jones, L.A., Dean, C.D., Mannion, P.D., Farnsworth, A., and Allison, P.A. (2021). Spatial sampling heterogeneity limits the detectability of deep time latitudinal biodiversity gradients. Proc. Biol. Sci. 288, 20202762. https://doi.org/10.1098/rspb.2020.2762.
- Jones, L.A., and Eichenseer, K. (2022). Uneven spatial sampling distorts reconstructions of Phanerozoic seawater temperature. Geology 50, 238–242. https://doi.org/10.1130/G49132.1.
- Close, R.A., Evers, S.W., Alroy, J., and Butler, R.J. (2018). How should we estimate diversity in the fossil record? Testing richness estimators using sampling-standardised discovery curves. Methods Ecol. Evol. 9, 1386– 1400. https://doi.org/10.1111/2041-210X.12987.
- Currie, P.J., and Koppelhus, E.B. (2005). Dinosaur Provincial Park: a Spectacular Ancient Ecosystem Revealed (Indiana University Press).
- Wagner, P.J., and Marcot, J.D. (2013). Modelling distributions of fossil sampling rates over time, space and taxa: assessment and implications for macroevolutionary studies. Methods Ecol. Evol. 4, 703–713. https:// doi.org/10.1111/2041-210X.12088.
- Starrfelt, J., and Liow, L.H. (2016). How many dinosaur species were there? Fossil bias and true richness estimated using a Poisson sampling model. Philos. Trans. R. Soc. Lond. B Biol. Sci. 371, 20150219. https:// doi.org/10.1098/rstb.2015.0219.
- MacKenzie, D.I., Nichols, J.D., Lachman, G.B., Droege, S., Andrew Royle, J., and Langtimm, C.A. (2002). Estimating site occupancy rates when detection probabilities are less than one. Ecology 83, 2248–2255. https://doi.org/10.1890/0012-9658(2002)083[2248:ESORWD]2.0.CO;2.
- MacKenzie, D.I., Nichols, J.D., Royle, J.A., Pollock, K.H., Bailey, L., and Hines, J.E. (2017). Occupancy Estimation and Modeling: Inferring Patterns and Dynamics of Species Occurrence (Elsevier).
- Liow, L.H., and Nichols, J.D. (2010). Estimating rates and probabilities of origination and extinction using taxonomic occurrence data: capturemark-recapture (CMR) approaches. Paleontol. Soc. Pap. 16, 81–94. https://doi.org/10.1017/S1089332600001820.
- 57. Schachat, S.R., Labandeira, C.C., Clapham, M.E., and Payne, J.L. (2019). A Cretaceous peak in family-level insect diversity estimated





- with mark-recapture methodology. Proc. Biol. Sci. 286, 20192054. https://doi.org/10.1098/rspb.2019.2054.
- Foote, M. (2016). On the measurement of occupancy in ecology and paleontology. Paleobiology 42, 707–729. https://doi.org/10.1017/pab. 2016 24
- Foote, M., Crampton, J.S., Beu, A.G., Marshall, B.A., Cooper, R.A., Maxwell, P.A., and Matcham, I. (2007). Rise and fall of species occupancy in Cenozoic fossil mollusks. Science 318, 1131–1134. https:// doi.org/10.1126/science.1146303.
- Kiessling, W., and Kocsis, Á.T. (2016). Adding fossil occupancy trajectories to the assessment of modern extinction risk. Biol. Lett. 12, 20150813. https://doi.org/10.1098/rsbl.2015.0813.
- Liow, L.H. (2013). Simultaneous estimation of occupancy and detection probabilities: an illustration using Cincinnatian brachiopods. Paleobiology 39, 193–213. https://doi.org/10.1666/12009.
- Lawing, A.M., Blois, J.L., Maguire, K.C., Goring, S.J., Wang, Y., and McGuire, J.L. (2021). Occupancy models reveal regional differences in detectability and improve relative abundance estimations in fossil pollen assemblages. Quat. Sci. Rev. 253, 106747. https://doi.org/10.1016/j. quascirev.2020.106747.
- 63. Chapman, B. (2021). Ecological Controls on the Campanian Distribution of Hesperornis (Aves: Hesperornithiformes) in the Western Interior Seaway. Master's Theses (Fort Hays State University).
- Reitan, T., Ergon, T.H., and Liow, L.H. (2023). Relative species abundance and population densities of the past: developing multispecies occupancy models for fossil data. Paleobiology 49, 23–38. https://doi.org/10.1017/pab.2022.17.
- Reitan, T., Martino, E.D., and Liow, L.H. (2024). Estimating relative species abundance using fossil data identified to different taxonomic levels. Ecography 2024, e06866. https://doi.org/10.1111/ecog.06866.
- Altwegg, R., and Nichols, J.D. (2019). Occupancy models for citizen-science data. Methods Ecol. Evol. 10, 8–21. https://doi.org/10.1111/2041-210X 13090
- Tingley, M.W., and Beissinger, S.R. (2009). Detecting range shifts from historical species occurrences: new perspectives on old data. Trends Ecol. Evol. 24, 625–633. https://doi.org/10.1016/j.tree.2009.05.009.
- Tingley, M.W., and Beissinger, S.R. (2013). Cryptic loss of montane avian richness and high community turnover over 100 years. Ecology 94, 598–609. https://doi.org/10.1890/12-0928.1.
- Jönsson, G.M., Broad, G.R., Sumner, S., and Isaac, N.J.B. (2021). A century of social wasp occupancy trends from natural history collections: spatiotemporal resolutions have little effect on model performance. Insect Conserv. Divers. 14, 543–555. https://doi.org/10.1111/jcad. 12494
- Shirey, V., Khelifa, R., M'Gonigle, L.K., and Guzman, L.M. (2023).
   Occupancy-detection models with museum specimen data: promise and pitfalls. Methods Ecol. Evol. 14, 402–414. https://doi.org/10.1111/ 2041-210X.13896.
- Wang, S.C., and Dodson, P. (2006). Estimating the diversity of dinosaurs.
   Proc. Natl. Acad. Sci. USA 103, 13601–13605. https://doi.org/10.1073/pnas.0606028103.
- Barrett, P.M., McGowan, A.J., and Page, V. (2009). Dinosaur diversity and the rock record. Proc. Biol. Sci. 276, 2667–2674. https://doi.org/ 10.1098/rspb.2009.0352.
- Johnston, A., Hochachka, W.M., Strimas-Mackey, M.E., Ruiz Gutierrez, V., Robinson, O.J., Miller, E.T., Auer, T., Kelling, S.T., and Fink, D. (2021). Analytical guidelines to increase the value of community science data: An example using eBird data to estimate species distributions. Divers. Distrib. 27, 1265–1277. https://doi.org/10.1111/ddi.13271.
- Cooper, R.B., Flannery-Sutherland, J.T., and Silvestro, D. (2024).
   DeepDive: estimating global biodiversity patterns through time using deep learning. Nat. Commun. 15, 4199. https://doi.org/10.1038/ s41467-024-48434-7.

- Benton, M.J. (2025). The dinosaur boom in the Cretaceous. Geol. Soc. Spec. Publ. 544, 453–475. https://doi.org/10.1144/SP544-2023-70.
- Rosenzweig, M.L. (1995). Species Diversity in Space and Time (Cambridge University Press). https://doi.org/10.1017/CBO9780511 623387
- Payne, J.L., and Finnegan, S. (2007). The effect of geographic range on extinction risk during background and mass extinction. Proc. Natl. Acad. Sci. USA 104, 10506–10511. https://doi.org/10.1073/pnas. 0701257104.
- Mace, G.M., Collar, N.J., Gaston, K.J., Hilton-Taylor, C., Akçakaya, H.R., Leader-Williams, N., Milner-Gulland, E.J., and Stuart, S.N. (2008). Quantification of Extinction Risk: IUCN's System for Classifying Threatened Species. Conserv. Biol. 22, 1424–1442. https://doi.org/10. 1111/j.1523-1739.2008.01044.x.
- Newsome, T.M., Wolf, C., Nimmo, D.G., Kopf, R.K., Ritchie, E.G., Smith, F.A., and Ripple, W.J. (2020). Constraints on vertebrate range size predict extinction risk. Glob. Ecol. Biogeogr. 29, 76–86. https://doi.org/10. 1111/qeb.13009.
- Royle, J.A., and Nichols, J.D. (2003). Estimating Abundance from Repeated Presence–Absence Data or Point Counts. Ecology 84, 777–790. https://doi.org/10.1890/0012-9658(2003)084[0777:EAFRPA]2. 0.CO;2.
- Brown, C.M., Evans, D.C., Campione, N.E., O'Brien, L.J., and Eberth, D.A. (2013). Evidence for taphonomic size bias in the Dinosaur Park Formation (Campanian, Alberta), a model Mesozoic terrestrial alluvialparalic system. Palaeogeogr. Palaeoclimatol. Palaeoecol. 372, 108–122. https://doi.org/10.1016/j.palaeo.2012.06.027.
- Brown, C.M., Campione, N.E., Wilson Mantilla, G.P.W., and Evans, D.C. (2022). Size-driven preservational and macroecological biases in the latest Maastrichtian terrestrial vertebrate assemblages of North America. Paleobiology 48, 210–238. https://doi.org/10.1017/pab.2021.35.
- Lyson, T.R., and Longrich, N.R. (2011). Spatial niche partitioning in dinosaurs from the latest cretaceous (Maastrichtian) of North America. Proc. Biol. Sci. 278, 1158–1164. https://doi.org/10.1098/rspb.2010.1444.
- Mallon, J.C., Evans, D.C., Ryan, M.J., and Anderson, J.S. (2012).
   Megaherbivorous dinosaur turnover in the Dinosaur Park formation (upper Campanian) of Alberta, Canada. Palaeogeogr. Palaeoclimatol. Palaeoecol. 350–352, 124–138. https://doi.org/10.1016/j.palaeo.2012.06.024
- Butler, R.J., and Barrett, P.M. (2008). Palaeoenvironmental controls on the distribution of Cretaceous herbivorous dinosaurs. Naturwissenschaften 95, 1027–1032. https://doi.org/10.1007/s00114-008-0417-5.
- Crees, J.J., Collen, B., and Turvey, S.T. (2019). Bias, incompleteness and the "known unknowns" in the Holocene faunal record. Philos. Trans. R. Soc. Lond. B Biol. Sci. 374, 20190216. https://doi.org/10.1098/rstb. 2019.0216.
- Antell, G.T., Benson, R.B.J., and Saupe, E.E. (2024). Spatial standardization of taxon occurrence data—a call to action. Paleobiology 50, 177–193. https://doi.org/10.1017/pab.2023.36.
- Holland, S.M. (2017). Structure, not Bias. J. Paleontol. 91, 1315–1317. https://doi.org/10.1017/jpa.2017.114.
- Husson, J.M., and Peters, S.E. (2018). Nature of the sedimentary rock record and its implications for Earth system evolution. Emerging Top. Life Sci. 2, 125–136. https://doi.org/10.1042/ETLS20170152.
- Zelenitsky, D.K., Therrien, F., Tanaka, K., Currie, P.J., and DeBuhr, C.L. (2017). Latest Cretaceous eggshell assemblage from the Willow Creek Formation (upper Maastrichtian lower Paleocene) of Alberta, Canada, reveals higher dinosaur diversity than represented by skeletal remains. Can. J. Earth Sci. 54, 134–140. https://doi.org/10.1139/cjes-2016-0080.
- Smith, A.B., Godsoe, W., Rodríguez-Sánchez, F., Wang, H.-H., and Warren, D. (2019). Niche Estimation Above and Below the Species Level. Trends Ecol. Evol. 34, 260–273. https://doi.org/10.1016/j.tree. 2018.10.012.

#### **Article**



- Castaño-Quintero, S., Escobar-Luján, J., Osorio-Olvera, L., Peterson, A.T., Chiappa-Carrara, X., Martínez-Meyer, E., and Yañez-Arenas, C. (2020). Supraspecific units in correlative niche modeling improves the prediction of geographic potential of biological invasions. PeerJ 8, e10454. https://doi.org/10.7717/peerj.10454.
- Chiarenza, A.A., Waterson, A.M., Schmidt, D.N., Valdes, P.J., Yesson, C., Holroyd, P.A., Collinson, M.E., Farnsworth, A., Nicholson, D.B., Varela, S., et al. (2023). 100 million years of turtle paleoniche dynamics enable the prediction of latitudinal range shifts in a warming world. Curr. Biol. 33, 109–121.e3. https://doi.org/10.1016/j.cub.2022.11.056.
- Outhwaite, C.L., Gregory, R.D., Chandler, R.E., Collen, B., and Isaac, N.J.B. (2020). Complex long-term biodiversity change among invertebrates, bryophytes and lichens. Nat. Ecol. Evol. 4, 384–392. https://doi. org/10.1038/s41559-020-1111-z.
- Erickson, K.D., and Smith, A.B. (2021). Accounting for imperfect detection in data from museums and herbaria when modeling species distributions: combining and contrasting data-level versus model-level bias correction. Ecography 44, 1341–1352. https://doi.org/10.1111/ecog. 05679.
- Hines, J.E., Nichols, J.D., Royle, J.A., MacKenzie, D.I., Gopalaswamy, A.M., Kumar, N.S., and Karanth, K.U. (2010). Tigers on trails: occupancy modeling for cluster sampling. Ecol. Appl. 20, 1456–1466. https://doi. org/10.1890/09-0321.1.
- Peters, S.E., and McClennen, M. (2016). The Paleobiology Database application programming interface. Paleobiology 42, 1–7. https://doi. org/10.1017/pab.2015.39.
- 98. R Core Team (2022). R: A Language and Environment for Statistical Computing. Version R Version 4.2.2 (R Foundation for Statistical Computing).
- Jones, L.A., Gearty, W., Allen, B.J., Eichenseer, K., Dean, C.D., Galván, S., Kouvari, M., Godoy, P.L., Nicholl, C.S.C., Buffan, L., et al. (2023). palaeoverse: A community-driven R package to support palaeobiological analysis. Methods Ecol. Evol. 14, 2205–2215. https://doi.org/10.1111/ 2041-210X.14099.
- Doser, J.W., and Stoudt, S. (2024). "Fractional replication" in single-visit multi-season occupancy models: impacts of spatiotemporal autocorrelation on identifiability. Methods Ecol. Evol. 15, 358–372. https://doi.org/ 10.1111/2041-210X.14275.
- Hijmans, R.J. (2023). raster: Geographic Data Analysis and Modeling.
   Version 3.6.26. https://cran.r-project.org/web/packages/raster/raster.pdf.
- 102. Valdes, P.J., Armstrong, E., Badger, M.P.S., Bradshaw, C.D., Bragg, F., Crucifix, M., Davies-Barnard, T., Day, J.J., Farnsworth, A., Gordon, C., et al. (2017). The BRIDGE HadCM3 family of climate models: HadCM3@Bristol v1. 0. Geosci. Model Dev. 10, 3715–3743. https://doi.org/10.5194/gmd-10-3715-2017.
- 103. Cox, M.D. (1984). A primitive equation, 3-dimensional model of the ocean. GFDL ocean group technical report 1. https://www.gfdl.noaa. gov/bibliography/related\_files/Cox\_1984\_GFDL\_Tech\_Report\_1.pdf
- 104. Kiehl, J.T., and Shields, C.A. (2013). Sensitivity of the Palaeocene– Eocene Thermal Maximum climate to cloud properties. Philos. Trans. A Math. Phys. Eng. Sci. 371, 20130093. https://doi.org/10.1098/rsta. 2013.0093.
- 105. Sagoo, N., Valdes, P., Flecker, R., and Gregoire, L.J. (2013). The Early Eocene equable climate problem: can perturbations of climate model parameters identify possible solutions? Philos. Trans. A Math. Phys. Eng. Sci. 371, 20130123. https://doi.org/10.1098/rsta.2013.0123.
- 106. Valdes, P.J., Scotese, C.R., and Lunt, D.J. (2020). Deep ocean temperatures through time. Clim. Past Discuss. 2020, 1–37.
- Scotese, C.R., and Wright, N. (2018). PALEOMAP paleodigital elevation models (PaleoDEMS) for the Phanerozoic. https://www.earthbyte.org/ paleodem-resource-scotese-and-wright-2018.
- Foster, G.L., Royer, D.L., and Lunt, D.J. (2017). Future climate forcing potentially without precedent in the last 420 million years. Nat. Commun. 8, 14845. https://doi.org/10.1038/ncomms14845.

- Gough, D.O. (1981). Solar Interior Structure and Luminosity Variations. In Physics of Solar Variations, V. Domingo, ed. (Springer Netherlands), pp. 21–34. https://doi.org/10.1007/978-94-010-9633-1\_4.
- 110. Chiarenza, A.A., Mannion, P.D., Farnsworth, A., Carrano, M.T., and Varela, S. (2022). Climatic constraints on the biogeographic history of Mesozoic dinosaurs. Curr. Biol. 32, 570–585.e3. https://doi.org/10.1016/j.cub.2021.11.061.
- Dean, C.D., Mannion, P.D., and Butler, R.J. (2016). Preservational bias controls the fossil record of pterosaurs. Palaeontology 59, 225–247. https://doi.org/10.1111/pala.12225.
- Dunne, E.M., Farnsworth, A., Greene, S.E., Lunt, D.J., and Butler, R.J. (2021). Climatic drivers of latitudinal variation in Late Triassic tetrapod diversity. Palaeontology 64, 101–117. https://doi.org/10.1111/pala.12514.
- 113. Oheim, K.B. (2007). Fossil site prediction using geographic information systems (GIS) and suitability analysis: The Two Medicine Formation, MT, a test case. Palaeogeogr. Palaeoclimatol. Palaeoecol. 251, 354–365. https://doi.org/10.1016/j.palaeo.2007.04.005.
- 114. Broxton, P.D., Zeng, X., Scheftic, W., and Troch, P.A. (2014). A MODIS-based global 1-km maximum green vegetation fraction dataset. J. Appl. Meteorol. Climatol. 53, 1996–2004. https://doi.org/10.1175/JAMC-D-13-0356.1
- Fick, S.E., and Hijmans, R.J. (2017). WorldClim 2: new 1-km spatial resolution climate surfaces for global land areas Fick. Int. J. Climatol. 37, 4302–4315.
- U.S. Geological Survey (2002). 1-Kilometer Resolution, North American Land Cover Characteristics, 1992-1993 (USGS). http://purl.stanford. edu/gk628xr0233 http://purl.stanford.edu/gk628xr0233.
- 117. Dunhill, A.M. (2012). Problems with using rock outcrop area as a paleon-tological sampling proxy: rock outcrop and exposure area compared with coastal proximity, topography, land use, and lithology. Paleobiology 38, 126–143. https://doi.org/10.1666/10062.1.
- 118. Peters, S.E., Husson, J.M., and Czaplewski, J. (2018). Macrostrat: A Platform for Geological Data Integration and Deep-Time Earth Crust Research. Geochem. Geophys. Geosyst. 19, 1393–1409. https://doi. org/10.1029/2018GC007467.
- 119. Lyster, S.J., Whittaker, A.C., Allison, P.A., Lunt, D.J., and Farnsworth, A. (2020). Predicting sediment discharges and erosion rates in deep time examples from the Late Cretaceous North American continent. Basin Res. 32, 1547–1573. https://doi.org/10.1111/bre.12442.
- Syvitski, J.P.M., and Milliman, J.D. (2007). Geology, Geography, and Humans Battle for Dominance over the Delivery of Fluvial Sediment to the Coastal Ocean. J. Geol. 115, 1–19. https://doi.org/10.1086/509246.
- 121. Watkins, S.E., Whittaker, A.C., Bell, R.E., McNeill, L.C., Gawthorpe, R.L., Brooke, S.A.S., and Nixon, C.W. (2019). Are landscapes buffered to highfrequency climate change? A comparison of sediment fluxes and depositional volumes in the Corinth Rift, central Greece, over the past 130 ky. GSA Bull. 131, 372–388. https://doi.org/10.1130/B31953.1.
- 122. Gearty, W., and Jones, L.A. (2023). rphylopic: An R package for fetching, transforming, and visualising PhyloPic silhouettes. Methods Ecol. Evol. 14, 2700–2708. https://doi.org/10.1111/2041-210X.14221.
- Isaac, N.J.B., van Strien, A.J., August, T.A., de Zeeuw, M.P., and Roy, D.B. (2014). Statistics for citizen science: extracting signals of change from noisy ecological data. Methods Ecol. Evol. 5, 1052–1060. https:// doi.org/10.1111/2041-210X.12254.
- 124. Outhwaite, C.L., Chandler, R.E., Powney, G.D., Collen, B., Gregory, R.D., and Isaac, N.J.B. (2018). Prior specification in Bayesian occupancy modelling improves analysis of species occurrence data. Ecol. Indic. 93, 333–343. https://doi.org/10.1016/j.ecolind.2018.05.010.
- 125. Plummer, M. (2003). JAGS: A program for analysis of Bayesian graphical models using Gibbs sampling. In Proceedings of the 3rd International Workshop on Distributed Statistical Computing, pp. 1–10.
- 126. August, T., Powney, G., Outhwaite, C., Harrower, C., Hill, M., Hatfield, J., Mancini, F., and Isaac, N. (2018). sparta: Trend analysis for unstructured





- data. R package version 0.1 40. https://biologicalrecordscentre.github. io/sparta/index.html.
- 127. Su, Y.-S., and Yajima, M. (2021). R2jags: Using R to Run "JAGS". R package version 0.7-1. https://CRAN.R-project.org/package=R2jags.
- 128. Gelman, A., and Rubin, D.B. (1992). Inference from iterative simulation using multiple sequences. Stat. Sci. 7, 457-472. https://doi.org/10. 1214/ss/1177011136.
- 129. Gelman, A., Carlin, J.B., Stern, H.S., and Rubin, D.B. (2014). Bayesian Data Analysis, Third Edition (Chapman and Hall/CRC).
- 130. Doser, J.W., Finley, A.O., Kéry, M., and Zipkin, E.F. (2022). spOccupancy: An R package for single-species, multi-species, and integrated spatial occupancy models. Methods Ecol. Evol. 13, 1670-1678. https://doi.org/10.1111/2041-210X.13897.
- 131. Polson, N.G., Scott, J.G., and Windle, J. (2013). Bayesian Inference for Logistic Models Using Pólya-Gamma Latent Variables. J. Am. Stat. Assoc. 108, 1339-1349. https://doi.org/10.1080/01621459.2013. 829001.
- 132. Datta, A., Banerjee, S., Finley, A.O., and Gelfand, A.E. (2016). Hierarchical Nearest-Neighbor Gaussian Process Models for Large Geostatistical Datasets. J. Am. Stat. Assoc. 111, 800-812. https://doi. org/10.1080/01621459.2015.1044091.
- 133. Watanabe, S. (2010). Asymptotic equivalence of Bayes cross validation and widely applicable information criterion in singular learning theory. J. Mach. Learn. Res. 11.
- 134. Fox, J., and Weisberg, S. (2018). An R Companion to Applied Regression (Sage Publications).

#### **Article**



#### **STAR**\*METHODS

#### **KEY RESOURCES TABLE**

REAGENT or RESOURCE	SOURCE	IDENTIFIER
Deposited data		
Dinosaur fossil occurrences, time bins, and geologic formation information used in this study; modelling results produced from this study.	Zenodo: https://doi.org/10.5281/zenodo.14946419	Supplementary_data
Paleobiology Database	https://paleobiodb.org	Accessed June 2024
Software and algorithms		
R scripts for analysis	https://doi.org/10.5281/zenodo.14946419	Supplementary_data
R computing environment	https://www.r-project.org/	Version 4.4.0
R package sparta	https://biologicalrecordscentre.github.io/sparta/index.html	Version 0.2.19
R package spOccupancy	https://cran.r-project.org/web/packages/spOccupancy/index.html	Version 0.7.6
R package sf	https://cran.r-project.org/web/packages/sf/index.html	Version 1.0.17
R package sp	https://cran.r-project.org/web/packages/sp/index.html	Version 2.1.4
R package raster	https://cran.r-project.org/web/packages/raster/index.html	Version 3.6.26
R package stars	https://cran.r-project.org/web/packages/stars/index.html	Version 0.6.5
R package MCMCvis	https://cran.r-project.org/web/packages/MCMCvis/index.html	Version 0.16.3
R package R2jags	https://cran.r-project.org/web/packages/R2jags/index.html	Version 0.8.5
R package snowfall	https://cran.r-project.org/web/packages/snowfall/index.html	Version 1.84.6.3
R package palaeoverse	https://palaeoverse.palaeoverse.org/index.html	Version 1.3.0
R package deeptime	https://cran.r-project.org/web/packages/deeptime/index.html	Version 1.1.1
R package rphylopic	https://cran.r-project.org/web/packages/rphylopic/index.html	Version 1.4.0
R package car	https://cran.r-project.org/web/packages/car/index.html	Version 3.1.2
R package ggplot2	https://ggplot2.tidyverse.org/	Version 3.5.1
R package rnaturalearth	https://cran.r-project.org/web/packages/rnaturalearth/index.html	Version 1.0.1

#### **METHOD DETAILS**

#### Occurrence dataset and data preparation

We downloaded a comprehensive dataset (>9000) of latest Cretaceous (Campanian–Maastrichtian, 83.6–66 million years before present [Ma]) North American terrestrial tetrapod fossil occurrences from the Paleobiology Database (PBDB; http://paleobiodb.org) on 12/06/2024. Stratigraphic ages were checked and standardised within the PBDB based on the recent literature. Occurrences without an associated stratigraphic formation and allochthonous occurrences were excluded prior to analysis, and ootaxa and ichnotaxa were also removed due to differences in taphonomic windows for preservation in comparison to body fossils. <sup>90</sup> We followed Chiarenza et al. <sup>18</sup> and focused on occurrences from four abundant and well-distributed clades of non-avian dinosaurs present in the latest Cretaceous of North America (Ankylosauridae, Ceratopsidae, Hadrosauridae, and Tyrannosauridae) which show relatively ecomorphologially comparable traits (e.g. body size, locomotion). Choosing families with abundant fossil material also ensured that there would be a sufficient number of successful detections of each clade for occupancy modelling to produce viable results. Despite concerns over the use of supra-specific taxonomic ranks within ecological niche modelling approaches, <sup>91</sup> families can provide valuable and informative data on macroevolutionary patterns at large scales. <sup>18,91–93</sup> The finalised dataset consists of 9186 total occurrences of terrestrial tetrapods from 2414 collections (visits), of which 1959 total occurrences (detections) were of the four targeted families (Ankylosauridae: 134; Ceratopsidae: 633; Hadrosauridae: 881; Tyrannosauridae: 311), found in 1374 total collections.

Occupancy modelling requires a site by observation matrix, with detection or non-detection of the target taxon being noted for each observation (e.g. a repeat visit to the site). These records of detection/non-detection per site are known as 'detection histories'. To enable the use of palaeontological data in occupancy modelling, we followed the occupancy structure suggested by Liow<sup>61</sup> and adapted by Lawing et al.<sup>62</sup> (Figure 1A) which uses palaeontological collections as visits, and the presence or absence of the target taxon within that collection as a detection or non-detection respectively. Similar approaches using lists of taxa collected at specific geographic coordinates have also been applied in studies utilising opportunistically collected data, such as for data gathered from



museum collections. 69,70,94,95 For those unfamiliar with occupancy modelling, we have provided a guide to some basic terms in Table S3. First, we generated raster layers of the North American continent at varying resolutions (see section 'temporal and spatial resolution' below for further information) to use individual grid cells of those layers as specific 'sites' within the occupancy modelling framework. Collections within each grid cell ('site') of the raster were treated as replicate 'visits' to that 'site', with the detection or non-detection of the targeted taxon within each collection being treated as the observation. 'Visits' are not inherently associated with temporality within the occupancy model framework, and instead can be unique geographic points within a broader 'site' 96. We opt to use this definition of 'visits', also known as the 'space-for-time substitution' in other occupancy modelling studies. 96 Palaeontological collections in the PBDB should represent separate collecting events tied to a specific geological time frame and geographic location, 97 and so fit the criteria for this definition of occupancy modelling 'visits'. We next had to convert our occurrence-based presence-only dataset into a presence/absence dataset suitable for occupancy modelling. To do this, we recorded whether the target taxon was present (1) or absent (0) within each collection/'visit' at each site, which was entered into the site by observation matrix. Note that using a dataset of all terrestrial tetrapod occurrences meant that we could record presences and absences of the target taxon in a larger number of 'sites' and associated 'visits' than if we were to just use a dataset of dinosaur occurrences. This approach is common-place when applying occupancy modelling to historic or citizen science data. When completed, each 'site' contains a history of detections/non-detections for individual 'visits'/collections at that 'site' (for example, a site might have a detection history of 101, indicating the target taxon was observed in one collection, not observed in a second collection, and then observed in a third collection). As we are only focussed on whether the target taxon is present or absent in a collection/'visit', this approach also means that taxonomic identification is only important for the target taxon, and more broadly for the chosen taxonomic rank of the target taxon. This significantly reduces the risk of taxonomic errors in the underlying dataset impacting results. Occurrence data from the PBDB were converted into formats suitable for multiple forms of occupancy modelling using newly devised custom functions in R (available in supplemental information).

Although occupancy models generally become more robust with a greater number of visits to sites (here, total number of collections per site) and sites do not need equal numbers of visits, datasets with a very large imbalance in the number of visits per site (e.g. a case where one site may have 80 visits, but all others have a maximum of 3 visits) can end up overemphasising the importance of highly visited sites when estimating the values of detection covariates, and can introduce potential bias from preferential sampling. The distribution of collections per cell in our data is right skewed, and so at all resolutions some cells would contain considerably more collections than others. Other studies have attempted to counteract the impacts of unequal numbers of visits/collections in opportunistically collected data by truncating the total number of visits/collections per site to a specific cap (e.g. 62,73). To resolve this issue for our dataset, we implemented a subsampling approach for visits/collections within occupancy models run with spOccupancy. We identified sites with a total number of visits/collections greater than a chosen maximum value, and then sampled visits from those sites without replacement to that chosen maximum value. We ran our spOccupancy models using these prepared sets of data to compare the impacts of this subsampling approach and varying numbers of visits on our results. We used 10 and 40 as the maximum numbers of visits for these models. These chosen values allow for comparison between a low limit that reduces the impact of sites containing many visits/collections but is also likely to show greater variability, versus a moderate limit that will be slightly more weighted towards sites with many visits/collections but is likely to have reduced overall variability in model results. All data preparation and modelling approaches were carried out in R version 4.2.2.98

#### **Temporal and spatial resolution**

The majority of occurrences from the Campanian–Maastrichtian WIB have been dated to stratigraphic stage level within the PBDB, which is a lower resolution than intended for use in this study. As such, we expanded on the formation dataset from Dean et al. <sup>19</sup> to more accurately assign temporal ranges to geological formations and their respective occurrences. Doing so reduced the possibility of assigning occurrences to incorrect time bins. This formation dataset consists of formations from the Late Cretaceous of North America, with associated maximum and minimum age, potential error of maximum and minimum age, depositional environment, information on methodology used to constrain ages, location, notes, and references for age constraints. Information was gathered from the available literature as well as Macrostrat (https://macrostrat.org). Diachronous formations were assigned a single maximum and minimum temporal limit. The finalised dataset consists of 122 total formations, with 58 from the WIB.

Occurrences were assigned maximum and minimum ages according to their associated formations. To align with the digital elevation models (DEMs) and palaeoclimatic data for occupancy models utilising explicit model covariates (described below), we used time bins based on the time intervals represented by the Scotese DEMs. These consist of four time bins, detailed in Table S4. For sparta occupancy models which did not require palaeoclimatic covariate data and so were not constrained to using the 'Scotese' time bins, we additionally used higher resolution time bins generated using the "Formation Binning" method of Dean et al. This approach uses the top and bottom ages of regional geological formations to assess the most suitable position for drawing interval boundaries, which produces higher resolution bins than those from the international commission of stratigraphy that are largely based on marine faunal turnover. It additionally allowed us to test how robust our results were to changes in bin length. We used a temporal window of 2.5 million years, which generated six unique bins. Details of bin lengths/intervals used within this study are available within Table S4. Occurrences were assigned to time bins using the 'majority' methodology of the bin\_time() function from the R package 'palaeoverse' ver. 1.2.1, and we removed any formations and associated occurrences that spanned across 3 or more bins to ensure that poorly-resolved occurrence didn't induce systematic error.



Occupancy models require a delicate balance between the number of sites visited versus the number of repeat visits to those sites: increased number of sites improves precision of occupancy estimates, but failure to conduct repeat surveys results in increased variance due to uncertainty around imperfect detection. <sup>55,100</sup> As the data used in this study were not purposefully collected for occupancy modelling, increasing the number of sites (in this case, increasing the resolution of grid cells which we used to generate our sites) will actively decrease the number of collections per site. To test for the impact of varying resolutions on model results, we generated grid cells according to two different resolutions: 0.5 degree and 1 degree (approximately 55.5 x 55.5 km, 111 x 111 km at the equator, respectively). In combination with the varying temporal resolutions, this approach allowed us to compare results and establish the optimal spatiotemporal resolution necessary for the study area (see 'occupancy modelling' section below for further details). Details on numbers of sites/visits for each model can be found in Table S5.

#### **Model covariates**

We selected a total of five variables to use as covariates for occupancy and seven variables for use in the detection parts of the occupancy model. These variables were chosen as they were expected to be important in shaping the distribution of dinosaur records across North America. Environmental layers were re-sampled to match the chosen resolution for the detection history data (see 'spatial' section above) and cropped to the chosen extent using the R package 'raster' ver. 3.6.26.<sup>101</sup> Modern environmental variable layers therefore were at a resolution of 0.5° or 1° and had an extent of 22.5–73°N and -155– -72°E. For present-day layers, covariate data were extracted per raster grid cell. For palaeogeographic layers where modern grid cells would not align with the positions of occurrences in deep time, fossil occurrences were palaeogeographically reconstructed using the 'point' method with the 'PALEO-MAP' model available within the 'palaeorotate' function from the 'palaeoverse' package ver. 1.2.1.<sup>99</sup> Covariate data were then extracted at each individual palaeogeographic locality, with the mean taken for all data within the same modern grid cell. Each variable we assessed was standardised to have a mean of 0 and standard deviation of 1 for each site, ensuring that estimated effect size was relative to the actual amount of variability in that covariate at that site.

#### Occupancy covariates

To explore the palaeoclimatic controls on dinosaur distribution we utilised a newly updated version of a state-of-the-art paleo-general circulation model. All palaeoclimate model simulations were carried out using a recent version of the UK MetOffice coupled Atmosphere-Ocean General Circulation Model (AOGCM), HadCM3 (specifically HadCM3L-M2.1D, following the nomenclature of Valdes et al.<sup>102</sup> HadCM3L-M2.1D has a model resolution of 3.75° longitude × 2.5° latitude in the atmosphere and ocean (~417 km × 278 km grid squares in the tropics), with 19 hybrid levels in the atmosphere and 20 vertical levels in the ocean with equations solved on the Arakawa B-grid. This resolution is coarser than our chosen study resolutions of 0.5° x 0.5° and 1° x 1°; however, this resolution represents the best readily available dataset for the chosen temporal resolution used in this study. Whilst this may have influenced the wide Bayesian credible intervals seen within occupancy covariates (e.g. Figures 5 and 6), climatic variables are consistently found as statistically significant covariates within our models, and as such are contributing important information to our models and subsequent interpretations. Sub-grid scale processes such as cloud, convection and oceanic eddies are parameterised as they cannot be resolved at the scales required (usually metres to several kilometres) of the model resolution. We use modern land surface vegetation (broadleaf trees, deciduous trees, shrubs, C3 and C4 grasses) and a globally uniform distribution of a medium loam soil characteristics in the model land surface scheme (MOSES 2.1) except for desert regions where the soil albedo is increased to that of sand. MOSES 2.1 also includes evaporation from sub-grid scale lakes (prescribed as a lake fraction for each grid box where present). We use a version of the model that includes the dynamical vegetation model TRIFFID (Top-Down Representation of Interactive Foliage and Flora Including Dynamics). TRIFFID predicts vegetation distributions of broadleaf trees, deciduous trees, shrubs, C3 and C4 grasses, in other words, Plant Functional Types (PFT) in the form of fractional coverage (and thus PFT co-existence) within a grid-cell. The fraction of each PFT is determined by competition equations based on their modern climate tolerances (predominantly temperature and precipitation). Each simulation was initialised from an equilibrated pre-industrial state in the atmosphere and ocean, referring to CO<sub>2</sub> at 280 ppm. Surface vegetation was uniformly set as shrub everywhere and then allowed to evolve via TRIFFID based on the evolution of the local climate. The ocean model is based on the model of Cox et al. 103 and is a full primitive equation, three-dimensional model of the ocean. Sea-ice is calculated on a zero-layer model with partial sea ice coverage possible with a consistent salinity assumed for ice.

The model used in this study has a further critical improvement from that of Valdes et al. <sup>102</sup> that raises higher latitude temperatures without significantly changing tropical temperatures reducing the pole-to-equator temperature gradient in line with proxy observations. <sup>104,105</sup> This update is also found to work under both hot, cool and icehouse conditions, as well as under pre-industrial boundary conditions making it appropriate for use across modern and deep time. The tropospheric height in these simulations' interactivity modifies the ozone scheme (set at pre-industrial values that change seasonally as a function of latitude and height) as warmer climates have a higher tropopause allowing ozone concentrations to similarly track this rise leading to greater surface warming (see Valdes et al. <sup>106</sup>).

Time-specific boundary conditions for four time intervals (80.8 Ma, 75.0 Ma, 69.0 Ma and 66.0 Ma; experiment codes teyeq, teyep, teyeo, teyen respectively) were constructed. Palaeogeographies (land-sea distribution, orography and bathymetry) were provided as part of the PALEOMAP project.<sup>107</sup> Each time specific digital elevation models were interpolated from a native 1° x 1° grid onto the HadCM3L 3.75° x 2.5° grid. 'Realistic' pCO<sub>2</sub> concentrations for each simulation are based on a multi-proxy compilation of Foster et al.<sup>108</sup> Solar luminosity for each simulation was based on Gough.<sup>109</sup> Orbital parameters and volcanic aerosol concentrations are kept at pre-industrial values.





To ensure each simulation has fully adjusted to the boundary conditions and is equilibrated, we follow a 3-stage spin-up protocol. i) The globally and volume-integrated annual mean ocean temperature trend is less than 1°C per 1000 years, ii) trends in surface air temperature are less than 0.3°C per 1000 years and iii) net energy balance at the top of the atmosphere, averaged over a 100-year period at the end of the simulation, is less than 0.25/W m². Climate means (i.e. mean annual temperature [MAT], mean annual precipitation [MAP], seasonal variation in temperature, and seasonal variation in precipitation) were produced from the last 100 years of the simulation.

Following the methodology of Chiarenza et al., <sup>18</sup> we included temperatures of the coldest and warmest quarters, precipitation of the driest and wettest quarters, and mean annual temperature standard deviation as suitable climatic variables that capture elements of seasonality. These measures were chosen due to being biologically meaningful and having previously (and subsequently <sup>110</sup>) shown to be important in determining dinosaur distributions across North America during the latest Cretaceous.

#### **Detection covariates**

Collections. The number of collections has been recognised as an important proxy for establishing relative sampling effort of vertebrate taxa in deep time, both temporally (e.g. Dean et al. 111) and spatially (e.g. Dunne et al. 112). To establish whether collection counts influenced detection probability, we calculated the number of collections per grid cell for each time interval and spatial resolution. This also allowed us to interrogate whether our models were impacted by uneven 'visits' per site (collections).

Distance from roads. Collecting fossils requires access to geological outcrop for both personnel and necessary equipment; consequently, the distance from the nearest road has been suggested as a proxy for accessibility and recovery of fossils. To test this, we downloaded a geospatial dataset of North American roads compiled by the U.S. Department of Transportation (https://data-usdot.opendata.arcgis.com/datasets/usdot::north-american-roads/about) and used the 'join attributes by nearest' tool of QGIS to find the distance from each collection from our dataset to the nearest road. This covariate was incorporated into the model as a site and survey-level variable, meaning that each collection contained an associated Distance value, rather than the site as a whole.

Maximum Green Vegetation Fraction (MGVF). Vegetative cover potentially prohibits the discovery of fossil material.<sup>24</sup> To test this we incorporated a continuous data set that represents the annual (rather than seasonal) maximum green vegetation fraction (0–100%) of each grid cell for North America, based on MODIS-derived normalised difference vegetation index data from 2001 to 2012 at 30 arc sec (~1-km) resolution.<sup>114</sup>

Modern rainfall. Rainfall may increase the probability of fossil discovery due to increased exposure from elevated erosion caused by surface runoff.<sup>36</sup> To test for this, modern climatic data was downloaded from WorldClim (www.worldclim.org), which provides average monthly climate data for minimum, mean, and maximum temperature and for precipitation for 1960–2000.<sup>115</sup> Data were downloaded for each month at a resolution of 30 arc seconds, and the mean taken across all months using the 'raster' package.

Land use. The composition of land cover within a given area could influence the potential to successfully recover fossil material. To investigate the potential impact of land use on occupancy, we utilised a 1km-resolution land cover dataset. These data were originally partitioned into 25 land cover types (see Table S6 for further information); these were simplified into the following four categories: 1) human altered landscapes, 2) open terrain, 3) forested terrain, 4) other. These data were re-sampled to match the associated resolution using the 'projectRaster' function of the 'raster' package, with method set to nearest neighbour, which is recommended for categorical variables.

Outcrop area. The available area of surficial geological outcrop that is both temporally relevant and fossil-bearing has been shown to influence diversity estimates in deep time, and generally acts as a limit on fossil recovery. <sup>18,117</sup> To test if outcrop area impacted detection probability, we acquired shapefiles of relevant Cretaceous geological outcrop matching our list of formations by accessing the Macrostrat API. <sup>118</sup> These shapefiles were then assigned to our four time bins using the bin\_time() function of the 'palaeoverse' package, using the associated temporal data from our formation list. Shapefiles for each time bin were combined within R and rasterized to the specified spatial resolution using the rasterize() function of the 'raster' package, with getCover set to TRUE to establish the percentage of each grid cell covered by outcrop.

Sediment flux. Chiarenza et al. 18 suggested that changes in sediment fluxes and surface run-off towards the end of the Cretaceous could have influenced the sampling of dinosaur fauna. To test this hypothesis, we estimated palaeo-sediment fluxes for the four major time intervals in this study. We followed the methodology of Chiarenza et al. 18 and Lyster et al. 119 who used palaeogeographic DEMs to reconstruct all catchments and associated palaeo-sediment fluxes across the entire North American continent. For each Scotese DEM, we used flow routing algorithms in the ArcGIS hydrological toolbox to delineate river catchments. Specifically, we used a D8 algorithm to create a flow direction network and the Basins tool to delineate catchments based on topographic highs in DEMs. 119 For each reconstructed catchment, we used zonal statistics to extract catchment geometries including area and maximum relief. Combining reconstructed catchments with HadCM3L GCM outputs, we also used zonal statistics to extract catchment-averaged climate variables including mean annual temperature and mean annual precipitation. With constraints on catchment geometries and catchment-averaged climate variables, we then used the BQART suspended sediment flux model 120 to estimate catchment palaeo-sediment fluxes. 18,119,121 BQART is an empirically-derived model of long-term (>30 year) mean annual suspended sediment fluxes 120 and, when applied to deep time studies, provides first-order estimates of palaeo-sediment fluxes. 119 BQART is particularly useful for reconstructing relative changes in palaeo-sediment fluxes, both in space and in time. 119 Full details of this methodology can be found in Lyster et al., 119 which includes discussion surrounding the sources and magnitudes of uncertainty in this methodology. We used BQART to calculate palaeo-sediment fluxes for each catchment, and we then converted the resulting shapefiles to rasters using the rasterize() function of the 'raster' package.



Random Effect. Covariates included within our model will not capture all potential factors influencing the detection of taxa, and thus will not capture all the spatial heterogeneity in detection probability between sites. To account for this issue, we included a random effect (intercept) varying by Site within the detection portion of our models (see below for further details).

#### **QUANTIFICATION AND STATISTICAL ANALYSIS**

#### **Occupancy modelling**

Occupancy modelling relies on sites within a geographic area being repeatedly sampled within a particular closed sampling window (season). Records of detections and non-detections during each visit at each site are used within the occupancy modelling framework to simultaneously estimate the probability of detection and the probability of occupancy, given the combination of detection histories observed. Occupancy models can additionally include either site- or visit-specific covariates which may influence either occupancy or detection parts of the model, and can be for an individual time frame (single-season) or span multiple time frames to produce estimates of occupancy and detection probability through time (multi-season, used in this work). Occupancy modelling is now commonplace in ecology and conservation, and thus specific details to the modelling process are not described here; further details can be found in Mackenzie et al. <sup>55</sup> Silhouettes were added to covariate forest plots using the 'rphylopic' package ver. 1.3.0, <sup>122</sup> and respective creators of the images are credited in said plots and in our acknowledgements.

#### Bayesian occupancy model

We first fit a multi-season (through time) Bayesian occupancy model framework based on Isaac et al. 123 and Outhwaite et al. 124 to compare naive occupancy against modelled estimates of occupancy and detection probability through time. These types of model have been shown to yield accurate and reliable species trends from presence-only records, even in situations with biased data, and have thus been determined as the most appropriate methodology for handling bias within unstructured occurrence record datasets. 123 The models were fitted using a Markov chain Monte Carlo (MCMC) algorithm in JAGS 125 via the function 'occDetFunc' from the R package 'sparta' ver. 0.2.19, 126 an R package containing various approaches for analysing unstructured occurrence records, and the package 'R2Jags' version 0.7.1.127 We ran two variants of the model. The first was run selecting the model-type 'sparta' with vague uninformative priors as specified by Isaac et al. 123 and using the categorical specification of 'list length', a proxy for sampling effort when modelling opportunistic biological records where detection probability is assumed to differ depending on whether a genus was observed on a shorter or longer list of total observed genera 123 (in this case, the total number of genera observed within a single palaeontological collection). The second was run using 'list length' alongside the random walk half-Cauchy prior approach of Outhwaite et al., 124 which improves occupancy estimates from datasets with lower number of records by sharing information between the current and previous years. Parameters set for the model included 40,000 iterations with a burn-in of 20,000, a thinning rate of 3, and 'n year' as 2, indicating any sites with fewer than two years of data to be dropped from the dataset. We assessed convergence of the parameter estimates from the MCMC chains using the Gelman-Rubin 'R-hat' statistic 128; all parameters converged at R-hat < 1.1. Species occupancy each year was calculated as a derived parameter within the model as the proportion of occupied sites. To assess whether our models were appropriately parameterized, we conducted posterior predictive checking, a Bayesian approach that assesses how well a model reproduces features of a dataset. 129 A data vector y<sub>rep</sub> is generated from the model fitted to the set of observations y; if the data are appropriately parameterized, the values of y and y<sub>rep</sub> should be similar. These checks should also provide assurance that the models have captured structures seen in the data and can be used reliably to make inferences about changes in occupancy and detection through time. Due to the binary nature of detection-nondetection data used in occupancy models, raw values must be binned and then a model fit assessment can be performed on the binned values. We followed the steps laid out in Outhwaite et al. 94 to produce summaries for two such checks: 1) the mean proportion of sites with detection records, averaged over all years; and 2) interannual variability, measured by the variance in the annual mean proportion of detections. Bayesian p-values were then calculated to establish whether there was a significant difference between the fitted data and original observations. These tests were implemented using custom script in R provided by Nick Isaac (pers. comms) and are provided within the supplemental information. Bayesian p-values for all bin types, spatial resolutions and taxonomic groups were above and below the threshold of significance (above 0.05 and below 0.95), indicating adequate model fit, except for hadrosauridae using formation bins at 0.5° resolution (full results can be found in Table S7).

#### Spatially-explicit multi-season occupancy model

We additionally used spatially-explicit multi-season (through time) occupancy models to assess the relative impacts of both fixed and random effects on occupancy and detection probability through time for our taxonomic groups. We fit our models with the 'spOccupancy' package <sup>130</sup> version 0.7.2, which uses a Markov chain Monte Carlo algorithm as well as Pólya-Gamma data augmentation for computational efficiency. <sup>131</sup> Occupancy models run using this package have an advantage over other commonly used occupancy modelling methods in that they can explicitly account for spatial autocorrelation and can include random effects within both occupancy and detection portions of the model. All models were fit using the stPGOcc() function in 'spOccupancy', which includes a Nearest Neighbour Gaussian Process <sup>132</sup> spatial random effect to account for spatial autocorrelation. Models additionally incorporated an AR(1) temporal random effect to account for potential temporal dependence between seasons (time bins). For all models run, parameter estimates were based on three chains, each with 20,000 iterations, a burn-in period of 10,000 iterations which are discarded, and a thinning rate of 10. We again used the Gelman–Rubin '*R*-hat' statistic <sup>128</sup> to assess whether or not the chains showed adequate convergence. We used the Widely Applicable Information Criterion <sup>133</sup> (WAIC) to compare the performance of the candidate models and determine the most supported predictors of occupancy and detection patterns. Covariates were assessed





for multicollinearity prior to modelling using the vif() function of the 'car' package, 134 with covariates exhibiting the largest variance inflation factor removed until all values were below 10. Only the occupancy variable of temperature of the coldest quarter was removed via this approach, which showed correlation with both temperature of the hottest quarter and mean annual temperature standard deviation. Due to the potential number of covariates available, we first modelled all combinations of detection covariates, holding occupancy constant using all potential covariates. The combination of detection covariates with the lowest WAIC was then held constant for the next set of models that explored combinations of occupancy covariates. Covariates of all top-ranked models were examined, and statistical significance was determined by comparing 95% credible intervals of the effect coefficients to zero. Bayesian analysis additionally permits the user to derive the probability of an effect being greater than 0, rather than just a binary significant/non-significant result. We carried out this approach for all models run and have highlighted traditionally non-significant covariates which show a 90% or greater chance of having an effect size greater than 0 (Table S2). To assess model fits, we used the posterior predictive checks included in the function ppcOcc() in the 'spOccupancy' package, grouping across both sites and replicate visits, and reported Bayesian p-values. Grouping the data across sites can help reveal whether the model fails to adequately represent variation in occurrence and detection probability across space, while binning the data across replicates/visits can show whether the model fails to adequately represent variation in detection probability across the different replicate visits (collections). We assumed values within the threshold of significance (above 0.05 and below 0.95) and relatively close to 0.5 indicated an adequate fit. Bayesian p-values for all families, resolutions and groupings were within this threshold indicating good model fit, except for Ankylosauridae at 0.5° capped at 40 visits for time bin one (80.8 Ma), Ceratopsidae at 1° capped at 40 visits for time bin two (75 Ma), and tyrannosauridae at 0.5° capped at 40 visits for time bin four (66.7 Ma), all when grouped across visits/collections (All results can be found in Table S8). Best fitting models were then used to additionally calculate detection probability throughout space and time using the fitted() function.

#### Spatiotemporal resolution tests

To test the impact of varying temporal and spatial resolution on our results, we ran a total of four models for each taxonomic grouping using the Bayesian sparta model discussed above: 1) Scotese bins (4 time bins), 0.5° resolution; 2) formation bins (6 time bins), 0.5° resolution; 3) Scotese bins (4 time bins), 1° resolution; 4) formation bins (6 time bins), 1° resolution. Tables reporting the number of sites/observations for each resolution, time bin and modelling approach are available in Table S5. To evaluate model performance, we followed the methodology of Jönsson et al.<sup>69</sup> by visually assessing occupancy and detection probability trends.